Title: A conditioned place preference for heroin is signaled by increased dopamine and direct pathway activity and decreased indirect pathway activity in the nucleus accumbens

Short title: Accumbens activity signals heroin conditioned place preference

Authors: Timothy J. O'Neal[1-4], Mollie X. Bernstein[1], Derek J. MacDougall[3], Susan M. Ferguson[2-4]

Affiliations: [1]Graduate Program in Neuroscience, University of Washington, Seattle, WA 98195
[2]Department of Psychiatry & Behavioral Sciences, University of Washington, Seattle, WA 98195
[3]Center for Integrative Brain Research, Seattle Children's Research Institute, Seattle, WA 98101
[4]Addictions, Drug & Alcohol Institute, University of Washington, Seattle, WA 98195

Contact info: Susan M. Ferguson (SMF) – smfergus@uw.edu

Conflict of interest statement: The authors declare no competing financial interests.

Acknowledgements: This work was supported by grants from the National Institute on Drug Abuse (F31DA047012 to TJO, R01DA036582 to SMF) and the UW Addictions, Drug & Alcohol Institute (ADAI-0138 to TJO). We thank Dr. John Neumaier and Dr. Michelle Kelly for providing the CAV2-Cre virus, the UW Molecular Genetics Resource Core (P30DA048736) for producing the AAV1-dLight1.3b virus, and Dr. Elizabeth Crummy, Dr. Scott Ng-Evans, and Joshua O'Neal for programming assistance.

ABSTRACT

Initial drug use promotes the development of conditioned reinforcement, whereby the reinforcing properties of a drug become attributed to drug-associated stimuli, such as cues and contexts. A principal role for the nucleus accumbens (NAc) in the response to drug-associated stimuli has been well-documented. In particular, direct and indirect pathway medium spiny neurons (dMSNs and iMSNs) have been shown to bidirectionally regulate cue-induced heroin-seeking in rats expressing addiction-like phenotypes, and a shift in NAc activity towards the direct pathway has been shown in mice following cocaine conditioned place preference (CPP). However, how NAc signaling guides heroin CPP, and whether heroin alters the balance of signaling between dMSNs and iMSNs remains unknown. Moreover, the role of NAc dopamine signaling in heroin reinforcement remains unclear. Here, we integrate fiber photometry for *in vivo* monitoring of dopamine and dMSN/iMSN calcium activity with a heroin CPP procedure in rats to address these outstanding questions. We identify a sensitization-like response to heroin in the NAc, with prominent iMSN activity during initial heroin exposure and prominent dMSN activity following repeated heroin exposure. We demonstrate a ramp in dopamine activity, dMSN activation, and iMSN inactivation preceding entry into a heroin-paired context, and a decrease in dopamine activity, dMSN inactivation, and iMSN activation preceding exit from a heroin-paired context. Finally, we show that buprenorphine is sufficient to prevent the development of heroin CPP and activation of the NAc post-conditioning. Together, these data support the hypothesis that an imbalance in NAc activity contributes to the development of addiction.

SIGNIFICANCE STATEMENT

The attribution of the reinforcing effects of drugs to neutral stimuli (e.g., cues and contexts) contributes to the maintenance of addiction, as re-exposure to drug-associated stimuli can reinstate drug seeking and taking even after long periods of abstinence. The nucleus accumbens (NAc) has an established role in encoding the value of drug-associated stimuli, and dopamine release into the NAc is known to modulate the reinforcing effects of drugs, including heroin. Using fiber photometry, we show that entering a heroin-paired context is driven by dopamine signaling and NAc direct pathway activation, whereas exiting a heroin-paired context is driven by NAc indirect pathway activation. This study provides further insight into the role of NAc microcircuitry in encoding the reinforcing properties of heroin.

INTRODUCTION

The opioid epidemic remains a major public health crisis in the United States, with relapse rates and overdose-related fatalities continuing to rise (Hedegaard et al., 2018). One critical mechanism underlying persistent drug-craving is conditioned drug reinforcement: the attribution of the reinforcing properties of a drug to a previously neutral stimulus (conditioned stimulus (CS); e.g., cues, contexts) (Everitt et al., 2018). Re-exposure to a drug-paired CS can reinstate drug-seeking following action/outcome devaluation (Shaham et al., 2003) or prolonged abstinence (Grimm et al., 2001). The nucleus accumbens (NAc) integrates cortical and subcortical inputs to guide behavioral processes associated with addiction, including associative learning, decision making, and motivation (Gerfen and Surmeier, 2011; Calabresi et al., 2014; Koob and Volkow, 2016). The NAc is heterogeneous, and predominantly comprised of two interspersed populations of medium spiny neurons (MSNs): direct pathway MSNs (dMSNs) that project to the ventral tegmental area (VTA) and primarily express the dopamine (DA) D1 receptor, and indirect pathway MSNs (iMSNs) that project to the ventral pallidum (VP) and primarily express the DA D2 receptor. These cell populations can have opposing control over behavioral output, with dMSNs serving as a “go” signal to facilitate behavioral actions and iMSNs serving as a “stop” signal to suppress or terminate unwanted actions (Albin et al., 1989; Kravitz et al., 2010; Cui et al., 2013; Macpherson et al., 2014). Moreover, emerging evidence has demonstrated a role for NAc dMSNs and iMSNs in encoding variability to the addictive effects of illicit drugs (Volkow et al., 2002; Nader et al., 2006; Belin et al., 2008; Bock et al., 2013; Yager et al., 2019; O’Neal et al., 2020), highlighting a central role for NAc MSNs in the transition to addiction.

Midbrain DA release into the NAc is central to the rewarding effects of illicit drugs (Crummy et al., 2020), and phasic DA release into the NAc promotes drug-seeking (Phillips et al., 2003). In addition to slower modulation of dMSNs and iMSNs via activation of G-protein coupled D1 and D2 receptors, DA can rapidly modulate these neuronal populations via opening of IP_3 receptors and release of intracellular Ca^{2+} (Swapna et al., 2016), a process that is integral for the propagation of Ca^{2+} waves and heterosynaptic plasticity in the NAc (Bailey et al., 2000; Plotkin et al., 2013). *In vivo* imaging of dMSN and iMSN Ca^{2+}

activity has revealed a rapid increase in dMSN activity and a progressive decrease in iMSN activity after acute cocaine exposure (Luo et al., 2011), as well as a persistent attenuation of iMSN activity after chronic cocaine treatment (Park et al., 2013); all of which lead to a long-lasting predominance of dMSN over iMSN signaling. Moreover, a ramping of dMSN Ca^{2+} activity along with a concomitant decrease in iMSN activity has been observed in mice preceding entry into a context associated with cocaine treatment (Calipari et al., 2016). Importantly, psychostimulants and opioids have different mechanisms of action and engage non-overlapping subcircuits to promote addictive behaviors (Badiani et al., 2011; Crummy et al., 2020), so the temporal relationship between NAc signaling and heroin-seeking remains unknown.

While targeted manipulations of dMSNs and iMSNs have demonstrated oppositional control over addictive behaviors (Lobo et al., 2010; Ferguson et al., 2011; O'Neal et al., 2020), it remains to be determined how the acquisition of a heroin CS is encoded by DA, dMSN, and iMSN signaling in the NAc. Thus, we combined fiber photometry for *in vivo* monitoring of NAc DA signaling and dMSN/iMSN Ca^{2+} signaling with a heroin conditioned place preference (CPP) procedure. NAc activity was recorded during early and late conditioning sessions to assess changes in the neural response over the course of conditioning. Following conditioning, we examined temporally precise DA signaling and activity of dMSNs and iMSNs during entries to and exits from contexts that had been paired with either saline or heroin and compared these signals with those recorded pre-conditioning. Finally, we explored the effects of buprenorphine, a partial mu opioid receptor agonist used in opioid-replacement therapy, on the acquisition of heroin CPP and subsequent activation of the NAc.

MATERIALS AND METHODS

Subjects

Outbred female (n = 40; ~8 weeks old, 175-199 g at arrival; Envigo) and male (n = 40; ~8 weeks old, 250-274 g at arrival; Envigo) Sprague-Dawley rats were pair-housed in a humidity- and temperature-controlled vivarium, with *ad libitum* access to food and water throughout the experiments. Rats were acclimated to the vivarium for at least five days and handled for at least three days prior to any procedures. All

procedures were done in accordance with the National Institutes of Health's Office of Laboratory Animal Welfare and were approved by the Seattle Children's Research Institute's Institutional Animal Care and Use Committee.

Drugs

Diamorphine HCl (heroin) was obtained through the Drug Supply Program of the National Institute on Drug Abuse (NIDA) and was dissolved in sterile saline (0.9%) to a concentration of 1-3 mg/ml and administered at a dose of 1 ml/kg. Buprenorphine was also obtained through the Drug Supply Program of NIDA and was dissolved in sterile saline (0.9%) to a concentration of 0.2 mg/ml and administered at a dose of 1 ml/kg.

Viral vectors

Adeno-associated viruses containing Flp recombinase (AAVrg-EF1a-flpo; #55637-AAVrg), Flp-dependent GCaMP6s (AAV8-EF1a-fDIO-GCaMP6s; #105714-AAV8), and Cre-dependent RCaMP1b (AAV1-Syn-FLEX-NES-jRCaMP1b-WPRE-SV40; #100850-AAV1) were acquired from Addgene and had titers of $\geq 1x10^{13}$ viral genomes/ml. dLight1.3b plasmid (AAV1-Syn-dLight1.3b) was acquired from Addgene (#135762) and prepared by the UW Molecular Genetics Resource Core. Canine adenovirus containing Cre recombinase (CAV2-Cre) had a titer of $\sim 2.5x10^{9}$ viral genomes/μl and was prepared as previously described (Kremer et al., 2009).

Stereotaxic surgery

Rats were anesthetized with isoflurane (3% induction, 1-2% maintenance; Patterson Veterinary) and injected with meloxicam (1 mg/ml, 1 ml/kg *sc*; Patterson Veterinary) for analgesia. Following head-fixation in a digital stereotax (Kopf Instruments), the skull was exposed and scored, and craniotomies were drilled above target nuclei. Viral vectors were loaded into 10 μl gas-tight syringes (Hamilton Company) and infused unilaterally into target nuclei (500 nl per virus, 100 nl/min). Coordinates (in mm, relative to Bregma (Paxinos et al., 1980)) were as follows: NAc [A/P +1.5, M/L +1.0, D/V -7.5], VP [A/P +0.2, M/L +2.0, D/V -

8.0], VTA [A/P -5.3, M/L +0.8 D/V -8.3]. To target dMSNs, AAVrg-EF1a-flpo was infused into the VTA and AAV8-EF1a-fDIO-GCaMP6s was infused into the NAc. To target iMSNs, CAV2-Cre was infused into the VP and AAV1-Syn-FLEX-NES-jRCaMP1b-WPRE-SV40 was infused into the NAc. Syringes were left in place for an additional 5 min following infusion and slowly retracted to allow proper diffusion of virus into target nuclei. Following viral infusion, fiber optic cannula (MFC_400/430-0.37_8mm_ZF2.5_FLT; >85% transmittance; Doric Lenses) were implanted in the NAc medial shell [D/V -7.4] and secured with skull screws, metabond (Patterson Dental), and dental cement.

Fiber photometry

Three weeks after surgery, fiber photometry recordings were performed using a multiplex photometry system (FP3001; Neurophotometrics Ltd., San Diego, CA). Rats were acclimated to branching fiber optic patch cords (BFP4_400/440/LWMJ-0.37_3m_SMA*-4xFC; Doric Lenses) for at least three days prior to testing, and biosensor expression was confirmed the day prior to testing via brief (~5 min) home cage recordings. For all recordings, LEDs were heated at 100% power for at least 5 min prior to recording to minimize heat-induced LED decay during recordings, then reduced to <50 μW for the duration of recordings (415 nm and 470 nm: ~12.5 μW; 560 nm: ~25 μW). Photometry recordings with a single biosensor (dLight1.3b imaging) used 2-phase cycling of 415 nm and 470 nm LEDs, and recordings with two biosensors (dual GCaMP6s/RCaMP1b imaging) used 3-phase cycling of 415 nm, 470 nm, and 560 nm LEDs. Fluorescent signals were bandpass filtered, collimated, reflected by a dichroic mirror, and focused by a 20x objective (0.40 NA) on the sensor of a CMOS camera. Signals were imaged at ~40 Hz, collected via custom-written workflows in Bonsai, and exported for off-line analysis via custom-written Python scripts.

Conditioned place preference

CPP apparatus

Behavioral sessions were conducted in custom-built acrylic chambers (TAP Plastics, Seattle, WA) with two equally sized but visually distinct chambers (15” wide x 15” long x 12” tall), and a smaller center

158 chamber (6" wide x 15" long x 12" tall) separated from the outer chambers via removable guillotine doors
159 (3" wide x 12" tall). The walls of the two outer chambers were covered with visually distinct wallpapers
160 (honeycomb and zebra, both grayscale), and the floor of the entire apparatus was matte black to facilitate
161 behavioral tracking. USB cameras (2.1mm, wide-angle; ELP) were positioned above CPP chambers and
162 interfaced with Bonsai for motion tracking. Video streams were greyscaled and thresholded, and binary
163 region analysis was used to detect animal position within the CPP chambers. Chambers were cleaned
164 between sessions with 70% ethanol (w/v).
165
166 *CPP procedure*
167 Experimental parameters were chosen based on a meta-analysis of heroin CPP by Bardo et al., 1995 to
168 maximize potential effect sizes. The overall CPP procedure included an initial preference test (15 min,
169 beginning at 11:00), eight conditioning sessions (2x/day, 40 min each, beginning at 09:00 and 13:00), and
170 a final preference test (15 min, beginning at 11:00). During the preference tests, the guillotine doors were
171 removed, and subjects were placed in the center of the neutral chamber and allowed to freely explore the
172 full apparatus. During conditioning sessions, subjects received *ip* injections of saline (morning) or heroin
173 (afternoon) and were immediately confined to one of the outer chambers. Saline and heroin pairings were
174 assigned in a pseudorandomized, counterbalanced design to avoid sex or treatment biases with either
175 chamber. Pretreatment injections of buprenorphine were given 10 min prior to injections of saline or
176 heroin, when appropriate. All behavioral testing was done during the light cycle, due to the use of visual
177 cues for conditioning.
178
179 **Immunohistochemistry**
180 After behavioral testing, rats were deeply anesthetized with Euthasol (2 ml/kg *ip*; 3.9 mg/ml pentobarbital
181 sodium and 0.5 mg/ml phenytoin sodium; Patterson Veterinary) and transcardially perfused with
182 phosphate-buffered saline (PBS; pH = 7.4) followed by paraformaldehyde (PFA; 4% in PBS). Brains were
183 extracted, fixed overnight in 4% PFA, post-fixed for >48 h in sucrose (30% in PBS), and sectioned (50
184 μm) with a vibrating microtome. Floating sections were washed (PBS; 3x10 min), blocked (0.25% Triton-

X, 5% normal goat serum, PBS; 2h), and incubated with primary antibodies (0.25% Triton-X, 2.5% normal goat serum, PBS; 24h) against Fos (1:800 rabbit anti-cFos, Cell Signaling #2250; RRID: AB_2247211) or tyrosine hydroxylase (1:400 mouse anti-TH, Sigma #MAB318; RRID: AB_2201528). Sections were then washed (PBS; 3x10 min) and incubated with secondary antibodies (0.25% Triton-X, 2.5% normal goat serum, PBS; 2h) conjugated to AF-568 (1:500 goat-anti-rabbit, Life Technologies #A11011; RRID: AB_143157) or AF-647 (1:500 goat-anti-mouse, Life Technologies #A21236; RRID: AB_2535805). Finally, sections were washed (PBS; 3x10min), mounted on slides, and cover-slipped with mounting medium with DAPI (Vectashield). Z-stacks along the rostral/caudal axis of the NAc (A/P +2.5 through A/P +0.7) were collected with confocal microscopy (20x; Zeiss LSM 710), and Fos^+ cells were quantified using ImageJ (V1.49; NIH) and Adobe Illustrator (CC 2020).

Experimental design and statistical analyses

Behavioral and photometry data were collected using custom-written workflows (Bonsai V3.5.2), processed using custom-written Python scripts (V3.7.7), and analyzed using Python and GraphPad Prism (V9.0). Transitions between chambers and cumulative time spent in each chamber were detected via binary region analysis in Bonsai and analyzed in Python. Heroin preference was calculated as the difference in time spent between chambers (i.e., Heroin preference = [time in heroin-paired] – [time in saline-paired]), and final preference was calculated as the change in preference across test sessions (i.e., CPP score = [Heroin preference, post-conditioning] – [Heroin preference, pre-conditioning]). Change in preference was analyzed using two-way repeated-measures (RM) ANOVA (dose x test) or two-tailed paired *t*-tests, and final preference was analyzed using one-way ANOVA. Equal numbers of female and male rats were included in each experiment, and sex differences in final preference were analyzed using two-way ANOVA (sex x dose) or two-tailed unpaired *t*-tests. Fos^+ cell counts along the rostral-caudal axis of the NAc were averaged into a single value per rat and analyzed using one-way ANOVAs or two-tailed unpaired *t*-tests for each subregion. Photometry signals were de-interleaved and corrected for photobleaching by fitting the isosbestic signal (415 nm) with a first-order exponential decay curve that was scaled and subtracted from experimental traces (Proulx et al., 2018; Martianova et al., 2019).

Linearized photometry traces were then converted to z-scores ($F_n - F_{mean} / F_{SD}$) using a rolling window of 10 s centered around F_n, and events were identified where $z > 2$ ($p < .05$) with a minimum inter-event interval of 1.5 s. Photometry signals during conditioning sessions were processed (event frequency, average amplitude, variance of amplitudes) and analyzed using two-way RM ANOVA (session x drug) and Kolmogorov-Smirnov tests (cumulative distribution of amplitudes). Photometry signals during test sessions were aligned to transitions between chambers, and the window centered around each transition (-3 s to +3 s) was extracted for analysis. Transition windows were analyzed using two-way RM ANOVA (time x test), the mean signal during transitions of each type were analyzed using two-tailed paired *t*-tests, and the cumulative signal during the transition window (area under the curve [AUC]) was calculated using trapezoidal numerical integration and analyzed using two-tailed paired *t*-tests. Statistical significance for all analyses was set at $p < .05$, and all ANOVAs were followed by Sidak *post-hoc* tests (behavioral and Fos data) or Benjamini and Hochberg FDR tests with $q < .05$ (photometry data). Data are shown throughout as individual subjects and/or mean ± SEM. Subjects with lack of viral expression ($n = 10$), incorrect fiber placement ($n = 4$), or no change in preference for the heroin-paired chamber ($n = 5$) were excluded from fiber photometry experiments.

RESULTS

Expression of heroin CPP is accompanied by robust activation of the NAc

Female and male rats underwent a heroin CPP procedure that included an initial preference test, four days of conditioning, and a final preference test (**Figure 1*A***). To identify a dose of heroin that would reliably produce a CPP, rats were conditioned with 0, 1, or 3 mg/kg heroin. A two-way RM ANOVA revealed a significant dose x test interaction on preference for the heroin-paired chamber ($F_{(2,21)} = 5.40$, $p = .013$), with rats conditioned with 3 mg/kg heroin significantly increasing time spent in the heroin-paired chamber on the post-test compared to the pre-test ($p = .023$; **Figure 1*B***). Moreover, a one-way ANOVA revealed a significant main effect of dose on final preference ($F_{(2,21)} = 5.28$, $p = .014$), with rats conditioned with 3 mg/kg heroin ($p = .0091$) but not 1 mg/kg heroin ($p = .078$) developing a stronger CPP for the heroin-paired chamber than rats conditioned with 0 mg/kg heroin (**Figure 1*C***). To assess the role

of the NAc in expression of a heroin CPP, rats were euthanized 30 min after the final preference test and brains were processed for Fos immunohistochemistry. An unpaired *t*-test revealed a significant effect of dose on Fos activation in the NAc core ($t_{(13)} = 3.54$, $p = .0036$), with significantly greater activation in rats conditioned with 3 mg/kg heroin (**Figure 1*D* – 1*E***). Similarly, an unpaired *t*-test revealed a significant effect of dose on Fos activation in the NAc shell ($t_{(13)} = 2.94$, $p = .012$), with significantly greater activation in rats conditioned with 3 mg/kg heroin (**Figure 1*F* – 1*G***). Importantly, two-way ANOVAs revealed no main effect of sex on final preference for the heroin-paired chamber ($F_{(1,18)} = 2.46$, $p = .13$) or Fos activation in the NAc core ($F_{(1,11)} = 0.0032$, $p = .96$) or NAc shell ($F_{(1,11)} = 2.17$, $p = .17$).

In vivo imaging of DA activity and MSN calcium activity in the NAc

To examine the role of NAc activity in the development and expression of a heroin CPP with temporal precision, CPP was coupled with fiber photometry for *in vivo* monitoring of DA signals, dMSN Ca^{2+} signals, and iMSN Ca^{2+} signals. Photometry signal quality was verified prior to starting CPP via brief home cage recordings from pairs of rats (**Figure 2*A* – 2*B***). Recordings were performed using either single-color photometry for DA imaging or dual-color photometry for simultaneous dMSN/iMSN Ca^{2+} imaging, with the isosbestic signal (415 nm) interleaved to correct for motion artifacts (**Figure 2*C***). DA imaging was performed with the DA sensor dLight1.3b (Patriarchi et al., 2018), a modified D1-type DA receptor with a cpGFP insert that expresses proximally to TH^+ DA terminals in the NAc (**Figure 2*D* – 2*F***). Dual dMSN/iMSN Ca^{2+} imaging was performed with the green-shifted and red-shifted Ca^{2+} indicators GCaMP6s and RCaMP1b, respectively, which were selectively targeted to dMSNs and iMSNs by infusing different retrogradely transported recombinases into the VTA (AAVrg-flpo to target dMSNs) and VP (CAV2-Cre to target iMSNs; **Figure 2*G***). GCaMP6s and RCaMP1b expression was detected throughout the NAc, with limited co-expression anywhere along the rostral/caudal axis (**Figure 2*H* – 2*I***). While the majority of rats co-expressed both indicators in the NAc ($n = 8$), a minority exclusively expressed GCaMP6s ($n = 4$) or RCaMP1b ($n = 2$); thus, for all MSN Ca^{2+} imaging experiments, GCaMP6s and RCaMP1b signals were independently analyzed. An overview of the analysis pipeline used for photometry signals is shown in **Figure 2*J***. Raw signals were de-interleaved to separate experimental

266 signals from the isosbestic signal, which was then used to linearize experimental signals and remove
267 motion artifacts. Linearized signals were converted to normalized z-scores using a rolling mean algorithm,
268 and significant upward deviations from the mean ("events") were detected in normalized signals and
269 extracted for additional analysis.
270
271 **The effects of heroin on DA, dMSN, and iMSN signaling change over the course of conditioning**
272 After confirming the quality of photometry signals, rats underwent heroin CPP with a 3 mg/kg conditioning
273 dose. NAc DA signals (n = 9), NAc dMSN Ca^{2+} signals (n = 12), or NAc iMSN Ca^{2+} signals (n = 10) were
274 recorded at four timepoints during conditioning: the saline and heroin pairings on the first day of
275 conditioning (session 1), and the saline and heroin pairings on the fourth day of conditioning (session 4;
276 **Figure 3*A* – 3*B***). For these recordings, pairs of rats were injected with saline or heroin, connected to the
277 photometry system via a branching fiber optic patch cord, and immediately placed into CPP chambers. As
278 recordings were not started until ~1min after rats received *ip* injections, analysis of photometry data was
279 done with a rolling window across the entirety of the conditioning session, rather than using a pre-
280 injection baseline period as a reference. A two-way RM ANOVA revealed a significant session x drug
281 interaction on the frequency of DA events ($F_{(1,8)}$ = 16.00, p = .004), with fewer DA events after heroin in
282 session 1 (saline 1 vs heroin 1, p = .017) but more DA events after heroin in session 4 (saline 4 vs heroin
283 4, p = .008; heroin 1 vs heroin 4, p = .0007; **Figure 3*C* – 3*D***). Kolmogorov-Smirnov tests on the
284 cumulative distribution of event amplitudes in each session revealed significant heroin-induced leftward
285 shifts in both session 1 (D = 0.18, p < .0001) and session 4 (D = 0.25, p < .0001), indicative of heroin-
286 induced suppression of large amplitude DA events (**Figure 3*E***). Indeed, two-way RM ANOVAs revealed
287 significant main effects of drug on both the mean amplitude of DA events ($F_{(1,8)}$ = 25.14, p = .001) and the
288 variance of DA event amplitudes ($F_{(1,8)}$ = 10.97, p = .011), with reduced amplitude (session 1, p = .017;
289 session 4, p = .0085) and variance (session 1, p = .0017; session 4, p = .008) of DA events after heroin
290 (**Figure 3*F* – 3*G***).
291

A two-way RM ANOVA on the frequency of dMSN Ca^{2+} events revealed a significant session x drug interaction ($F_{(1,11)}$ = 12.96, p = .0042) with a selective reduction in dMSN signaling events during the fourth saline session (saline 1 vs saline 4, p = .0016), suggesting heroin-induced disruption in the basal level of dMSN Ca^{2+} signaling (**Figure 3*H* – 3*I***). Kolmogorov-Smirnov tests on the cumulative distribution of dMSN event amplitudes revealed significant heroin-induced leftward shifts in both session 1 (D = 0.53, p < .0001) and session 4 (D = 0.46, p < .0001), indicative of heroin-induced suppression of large amplitude dMSN signaling events (**Figure 3*J***). Accordingly, a two-way RM ANOVA revealed a significant main effect of drug on the mean amplitude of dMSN events ($F_{(1,11)}$ = 17.49, p = .0015) but not the variance of dMSN event amplitudes ($F_{(1,11)}$ = 1.03, p = .33), with significant heroin-induced reductions in amplitude in both session 1 (p = .011) and session 4 (p = .0043; **Figure 3*K* – 3*L***).

A two-way RM ANOVA on the frequency of iMSN Ca^{2+} events revealed a significant session x drug interaction ($F_{(1,9)}$ = 19.11, p = .0018), with an increase in iMSN events after heroin in session 1 (saline 1 vs heroin 1, p = .0073) but a decrease in iMSN events after heroin in session 4 (saline 4 vs heroin 4, p = .023; heroin 1 vs heroin 4, p = .0009; **Figure 3*M* – 3*N***). Moreover, Kolmogorov-Smirnov tests on the cumulative distribution of iMSN event amplitudes revealed a heroin-induced rightward shift in session 1 (D = 0.49, p < .0001), but a leftward shift in session 4 (D = 0.42, p < .0001; **Figure 3*O***). A two-way RM ANOVA on the mean amplitude of iMSN events revealed both a significant main effect of session ($F_{(1,9)}$ = 8.37, p = .018) and a significant session x drug interaction ($F_{(1,9)}$ = 14.76, p = .004), with greater iMSN amplitudes after heroin in session 1 (saline 1 vs heroin 1, p = .0034) but weaker iMSN amplitudes after heroin in session 4 (heroin 1 vs heroin 4, p < .0001; **Figure 3*P***). However, two-way RM ANOVAs on the variance of iMSN event amplitudes found no significant main effect of drug ($F_{(1,9)}$ = 1.76, p = .22) and no significant session x drug interaction ($F_{(1,9)}$ = 2.07, p = .18; **Figure 3*Q***).

NAc DA signaling increases when entering and decreases when exiting a heroin-paired context

Photometry signals were also recorded during both the initial (“pre-test”) and final (“post-test”) preference tests to assess the role of NAc DA signaling in the expression of a heroin CPP (**Figure 4*A* – 4*B***). A paired

319 *t*-test revealed a significant increase in preference for the heroin-paired chamber during the post-test
320 compared to the pre-test ($t_{(8)} = 5.35$, $p = .0007$; **Figure 4*C***), and an unpaired *t*-test found no sex
321 difference in final preference for the heroin-paired chamber ($t_{(7)} = 0.51$, $p = .62$; data not shown).
322 Transitions between the center chamber and the saline- and heroin-paired chambers were timestamped
323 and aligned to photometry signals, and the window centered around each transition (-3 s to +3 s) was
324 isolated for analysis. A two-way RM ANOVA revealed a significant time x test interaction during entries to
325 the saline-paired chamber ($F_{(119,952)} = 1.30$, $p = .023$), with significantly weaker DA signaling in the 0.5 s
326 centered around entry in the post-test ($p < .008$; **Figure 4*D***). Moreover, paired *t*-tests found significantly
327 weaker DA signaling at the moment of entry ($t_{(8)} = 4.62$, $p = .0017$) as well as across the entire entry
328 window ($t_{(8)} = 3.94$, $p = .0043$) in the post-test (**Figure 4*E* – 4*F***). However, a two-way RM ANOVA
329 revealed no significant time x test interaction during exits from the saline-paired chamber ($F_{(119,952)} = 1.12$,
330 $p = .19$), and paired *t*-tests found no significant difference in DA signaling at the moment of exit ($t_{(8)} =$
331 0.63, $p = .55$) or across the exit window ($t_{(8)} = 0.31$, $p = .76$) in the post-test (**Figure 4*G* – 4*I***). Conversely,
332 a two-way RM ANOVA revealed a significant time x test interaction during entries to the heroin-paired
333 chamber ($F_{(119,952)} = 13.01$, $p < .0001$), with significantly greater DA signaling in the 1s centered around
334 entry in the post-test ($p < .008$; **Figure 4*J***). Additionally, paired *t*-tests found significantly larger DA signals
335 at the moment of entry to the heroin-paired chamber ($t_{(8)} = 6.70$, $p = .0002$) as well as across the entire
336 entry window ($t_{(8)} = 6.47$, $p = .0002$) in the post-test (**Figure 4*K* – 4*L***). Finally, a two-way RM ANOVA
337 revealed a significant time x test interaction during exits from the heroin-paired chamber ($F_{(119,952)} = 3.04$,
338 $p < .0001$), with significantly stronger DA signaling ~2 s preceding exit ($p < .004$) but significantly weaker
339 DA signaling in the 1 s centered around exit ($p < .003$) in the post-test (**Figure 4*M***). Paired *t*-tests also
340 found significantly weaker DA signals at the moment of exit from the heroin-paired chamber ($t_{(8)} = 7.19$, p
341 $< .0001$) but no difference in the DA signal across the entire exit window ($t_{(8)} = 0.0064$, $p > 0.99$) in the
342 post-test (**Figure 4*N* – 4*O***).
343
344 **NAc dMSN signaling increases when entering and decreases when exiting a heroin-paired context**

Photometry signals were also recorded during the preference tests to assess the role of NAc dMSN signaling in the expression of a heroin CPP (**Figure 5*A* – 5*B***). A paired *t*-test revealed a significant increase in preference for the heroin-paired chamber during the post-test compared to the pre-test ($t_{(11)}$ = 3.17, p = .009; **Figure 5*C***), and an unpaired *t*-test found no sex difference in final preference for the heroin-paired chamber ($t_{(10)}$ = 0.16, p = .88; data not shown). A two-way RM ANOVA revealed a significant time x test interaction during entries to the saline-paired chamber ($F_{(79,869)}$ = 5.26, p < .0001), with significantly weaker dMSN signaling from 1 s preceding to 1.5 s following entry (p < .008) in the post-test (**Figure 5*D***). Moreover, paired *t*-tests found significantly weaker dMSN signaling at the moment of entry ($t_{(11)}$ = 5.83, p = .0001) as well as across the entire entry window ($t_{(11)}$ = 3.26, p = .0076) in the post-test (**Figure 5*E* – 5*F***). However, a two-way RM ANOVA revealed no significant time x test interaction during exits from the saline-paired chamber ($F_{(79,869)}$ = 1.27, p = .063), and paired *t*-tests found no significant difference in dMSN signaling at the moment of exit ($t_{(11)}$ = 0.20, p = .84) or across the exit window ($t_{(11)}$ = 0.069, p = .95) in the post-test (**Figure 5*G* – 5*I***). Conversely, a two-way RM ANOVA revealed a significant time x test interaction during entries to the heroin-paired chamber ($F_{(79,869)}$ = 18.71, p < .0001), with significantly greater dMSN signaling in the 2 s centered around entry in the post-test (p < .002; **Figure 5*J***). Additionally, paired *t*-tests found significantly larger dMSN signals at the moment of entry to the heroin-paired chamber ($t_{(11)}$ = 9.34, p < .0001) as well as across the entire entry window ($t_{(11)}$ = 3.87, p = .0026) in the post-test (**Figure 5*K* – 5*L***). Finally, a two-way RM ANOVA revealed a significant time x test interaction during exits from the heroin-paired chamber ($F_{(79,869)}$ = 5.78, p < .0001), with significantly weaker dMSN signaling in the 1 s centered around exit (p < .002) in the post-test (**Figure 5*M***). Paired *t*-tests also found significantly weaker dMSN signals at the moment of exit from the heroin-paired chamber ($t_{(11)}$ = 6.29, p < .0001) but no difference in the dMSN signal across the entire exit window ($t_{(11)}$ = 2.00, p = 0.071) in the post-test (**Figure 5*N* – 5*O***).

NAc iMSN signaling decreases when entering and increases when exiting a heroin-paired context

Photometry signals were also recorded during the preference tests to assess the role of NAc iMSN signaling in the expression of a heroin CPP (**Figure 6*A* – 6*B***). A paired *t*-test revealed a significant

increase in preference for the heroin-paired chamber during the post-test compared to the pre-test ($t_{(10)}$ = 3.28, p = .0084; **Figure 6*C***), and an unpaired *t*-test found no sex difference in final preference for the heroin-paired chamber ($t_{(8)}$ = 0.42, p = .68; data not shown). A two-way RM ANOVA revealed a significant time x test interaction during entries to the saline-paired chamber ($F_{(79,711)}$ = 2.88, p < .0001), with significantly stronger iMSN signaling from 0.5 s preceding to 1.5 s following entry (p < .006) in the post-test (**Figure 6*D***). Moreover, paired *t*-tests found significantly greater iMSN signaling at the moment of entry ($t_{(9)}$ = 3.50, p = .0067) as well as across the entire entry window ($t_{(9)}$ = 2.32, p = .045) in the post-test (**Figure 6*E* – 6*F***). However, a two-way RM ANOVA revealed no significant time x test interaction during exits from the saline-paired chamber ($F_{(79,711)}$ = 0.67, p = .99), and paired *t*-tests found no significant difference in iMSN signaling at the moment of exit ($t_{(9)}$ = 1.33, p = .22) or across the exit window ($t_{(9)}$ = 2.23, p = .053) in the post-test (**Figure 6*G* – 6*I***). Conversely, a two-way RM ANOVA revealed a significant time x test interaction during entries to the heroin-paired chamber ($F_{(79,711)}$ = 2.40, p < .0001), with significantly weaker iMSN signaling in the 1 s centered around entry in the post-test (p < .003; **Figure 6*J***). Additionally, paired *t*-tests found significantly smaller iMSN signals at the moment of entry to the heroin-paired chamber ($t_{(9)}$ = 2.55, p = .031) as well as across the entire entry window ($t_{(9)}$ = 3.64, p = .0054) in the post-test (**Figure 6*K* – 6*L***). Finally, a two-way RM ANOVA revealed a significant time x test interaction during exits from the heroin-paired chamber ($F_{(79,711)}$ = 1.63, p = .0008), with significantly stronger iMSN signaling in the 1 s centered around exit (p < .006) in the post-test (**Figure 6*M***). Paired *t*-tests also found significantly stronger iMSN signals at the moment of exit from the heroin-paired chamber ($t_{(9)}$ = 3.57, p = .006) as well as across the entire exit window ($t_{(9)}$ = 3.53, p = 0.0064) in the post-test (**Figure 6*N* – 6*O***).

Buprenorphine pretreatment blocks the development of heroin CPP

Buprenorphine is used for opioid replacement therapy due to its ability to weakly activate mu opioid receptor signaling and prevent the binding of other opioids (e.g., heroin), and was recently shown to occlude heroin-evoked DA release into the NAc (Isaacs et al., 2020). To determine whether buprenorphine could similarly prevent the acquisition of heroin CPP, rats underwent a modified CPP

399 procedure with 0 or 0.2 mg/kg buprenorphine given 10 min prior to each conditioning session (**Figure**
400 **7*A***). A two-way RM ANOVA revealed a significant dose x test interaction on heroin preference ($F_{(1,14)}$ =
401 8.52, p = .012), with a significant increase in time spent in the heroin-paired chamber for rats pretreated
402 with 0 mg/kg buprenorphine (p = .0086) but not 0.2 mg/kg buprenorphine (p = .73; **Figure 7*B***). Moreover,
403 an unpaired *t*-test revealed significantly lower final preference for the heroin-paired chamber in rats
404 pretreated with 0.2 mg/kg buprenorphine ($t_{(14)}$ = 2.83, p = .014; **Figure 7*C***). To assess the impact of
405 buprenorphine pretreatment during conditioning on NAc activation during the final preference test, rats
406 were euthanized 30 min after the final preference test and brains were processed for Fos
407 immunohistochemistry. Unpaired *t*-tests revealed significantly lower levels of Fos activation in both the
408 NAc core ($t_{(14)}$ = 4.78, p = .0003) and NAc shell ($t_{(14)}$ = 6.20, p < .0001) for rats pretreated with 0.2 mg/kg
409 buprenorphine during conditioning (**Figure 7*D*– 7*G***). Importantly, two-way ANOVAs revealed no main
410 effect of sex on final preference for the heroin-paired chamber ($F_{(1,12)}$ = 1.40, p = .26) or Fos activation in
411 the NAc core ($F_{(1,12)}$ = 1.09, p = .32) or NAc shell ($F_{(1,12)}$ = 0.26, p = .62).
412
413 **DISCUSSION**
414 Here, we sought to examine the role of NAc signaling in the acquisition and expression of heroin CPP by
415 coupling fiber photometry recordings with a heroin CPP procedure that induces Fos activation in the NAc
416 during expression of heroin CPP. We identified differences in the neural response to heroin over the
417 course of conditioning, with suppression of NAc activity during early conditioning but enhancement of NAc
418 activity during late conditioning. Next, we demonstrated that entering a heroin-paired context is
419 accompanied by increased dopamine and dMSN Ca^{2+} signaling along with decreased iMSN Ca^{2+}
420 signaling, while exiting a heroin-paired context is accompanied by increased iMSN signaling along with
421 decreased dopamine and dMSN signaling. Finally, we show that buprenorphine pretreatment during
422 conditioning is sufficient to prevent the expression of heroin CPP and concomitant activation of the NAc.
423 Together, these data reveal a central role for the NAc in the reinforcing effects of heroin, in accordance
424 with the hypothesis that an imbalance in signaling between the accumbal direct and indirect pathways
425 drives addictive behaviors.

Dopaminergic modulation in the NAc contributes to heroin conditioning

While the contribution of DA to the rewarding effects of most potentially addictive drugs (e.g., psychostimulants, nicotine) is well-established (Crummy et al., 2020), the role of DA in opioid reward is more complicated (Badiani et al., 2011). Opioids increase phasic DA release, and both D1 receptor blockade and D2 receptor deletion blocks morphine reward (Johnson and North, 1992; Shippenberg et al., 1993; Maldonado et al., 1997; Sellings and Clarke, 2003). However, bilateral 6-OHDA lesions of the NAc can block or have no effect on morphine reward (Shippenberg et al., 1993; Sellings and Clarke, 2003), and chronic blockade of both D1 and D2 receptors potentiates the rewarding effects of low doses of heroin (Stinus et al., 1989). During conditioning, we identified noteworthy effects of heroin on DA signaling: a significant reduction in large amplitude DA events during both early and late conditioning sessions, a significant reduction in the frequency of DA events during early conditioning, and a significant enhancement in the frequency of DA events during late conditioning. This shift from suppression to elevation across conditioning suggests sensitization of the dopaminergic response to heroin and supports a role for DA in the acquisition of heroin CPP. After conditioning, we detected a significant increase in DA signaling preceding entries to the heroin-paired chamber, as well as significant decreases in DA signaling preceding exits from the heroin-paired chamber and entries to the saline-paired chamber, indicating emergent selectivity for DA signaling in response to a heroin-paired context. Notably, a recent study using DA imaging in the NAc medial shell following heroin administration reported a significant rise in tonic DA signaling over a period of minutes, relative to a pre-injection baseline (Corre et al., 2018). We did not observe a similar effect on DA signaling during conditioning, although we believe this is largely due to lack of a pre-injection baseline in the study design. Future work will expand upon this data to better understand how heroin conditioning is altering tonic signaling in the NAc, in addition to phasic changes.

An imbalance in accumbal activity develops during heroin conditioning

The ability of DA to alter overall accumbal activity is dependent not only on dopaminergic modulation of individual MSNs but also on the network implications of such modulation. Although dMSNs and iMSNs

453 can be differentiated according to their downstream targets (VTA and VP, respectively), both subtypes of
454 MSNs are heavily interconnected in a local microcircuit of lateral inhibition within the NAc (Burke et al.,
455 2017). Indeed, although dMSNs are more likely to collateralize with other dMSNs than iMSNs (Taverna et
456 al., 2008), D2 receptor-mediated disinhibition of iMSN lateral inhibition onto dMSNs is necessary for the
457 locomotor sensitizing effects of cocaine (Dobbs et al., 2016). An imbalance between dMSNs and iMSNs
458 can thereby shape the ability of DA to modulate accumbal activity, with the overall balance in signaling
459 guiding vulnerability to the reinforcing effects of drugs.
460
461 We observed a shift in the response of NAc iMSNs to heroin over the course of conditioning, with a
462 prominence of iMSN signaling during early conditioning (enhanced iMSN frequency and amplitudes) and
463 a suppression of iMSN signaling during late conditioning (reduced iMSN frequency and amplitudes). This
464 inhibition of iMSN signaling – mediated in part by an enhanced dopaminergic response to heroin during
465 late conditioning – would release nearby dMSNs from tonic lateral inhibition, allowing direct pathway
466 signaling to dominate. Interestingly, however, we did not observe a sensitized dMSN response to heroin
467 over the course of conditioning; rather, we observed a transient reduction in dMSN signaling during the
468 fourth saline session, indicating a weakening of basal dMSN tone over the course of heroin conditioning.
469 In addition to heroin-induced disruptions in NAc activity over the course of conditioning, we identified
470 context-dependent changes in MSN signals post-conditioning. dMSN signals were significantly stronger
471 when entering the heroin-paired context, but significantly weaker when exiting the heroin-paired or
472 entering the saline-paired contexts. Conversely, iMSN signals were significantly weakened when entering
473 the heroin-paired context, but significantly stronger when exiting the heroin-paired or entering the saline-
474 paired contexts. These data indicate selective tuning of dMSNs to the heroin-paired context, and are in
475 consistent with previous findings of elevated dMSN signaling during re-exposure to a cocaine-paired
476 context (Calipari et al., 2016).
477
478 **Disrupting opioid signaling prevents development of heroin CPP**

In our final experiment, we show that pretreatment with buprenorphine during conditioning blocked the development of a heroin CPP and associated Fos activity in the NAc. Although buprenorphine weakly activates mu opioid receptors to mildly elevate DA release, it also prevents heroin from binding to the same receptors and driving larger phasic DA release (Isaacs et al., 2020). The buprenorphine dose used in the present study was selected based on a previous report that described a bell-shaped curve for buprenorphine-stimulated DA release into the NAc: significant increases in DA release with 0.01 – 0.04 mg/kg buprenorphine, but no change in DA release with 0.18 – 0.7 mg/kg buprenorphine (Isaacs et al., 2020). Moreover, twice daily injections of 0.1 – 0.4 mg/kg buprenorphine were sufficient to significantly attenuate cocaine self-administration in rats, with no differences observed between 0.1 and 0.4 mg/kg (Carroll and Lac, 1992). Thus, our dose of buprenorphine administered prior to each conditioning session likely produced comparably low levels of DA release in both chambers, preventing the acquisition of a strong conditioned response to heroin.

Technical considerations

Although dMSNs and iMSNs have canonically been assumed to project exclusively to the VTA and VP, respectively, growing evidence has demonstrated that dMSNs project equally strong to the VTA and the VP (Kupchik et al., 2015; Creed et al., 2016). Importantly, the viral strategy used here has been shown to target largely non-overlapping populations of neurons in the NAc with bidirectional control over cue-induced heroin-seeking (O'Neal et al., 2020). In the present study we not only did not observe co-expression of GCaMP6s and RCaMP1b within the NAc, but we also observed oppositional dMSN and iMSN signals during transitions in the post-test, similar to what has previously been reported during cocaine CPP (Calipari et al., 2016). Furthermore, although dual-color imaging runs the risk of signal crosstalk and contamination (Meng et al., 2018), our dMSN-GCaMP6s and iMSN-RCaMP1b signals were highly uncorrelated throughout testing (pre-conditioning r^2: mean = 0.02, range = $3.4e^{-7}$ to 0.08; post-conditioning r^2: mean = 0.05, range = $4.0e^{-3}$ to 0.17). Additionally, there is concern that the viral strategy used to target dMSNs may have led to undesired expression of GCaMP6s in DA terminals in the NAc. While retrograde AAVs have a higher tropism for axon terminals, some evidence has suggested they may

506 also infect cell bodies at the site of infusion (Tervo et al., 2016); moreover, AAV8s have been shown to
507 undergo some degree of retrograde transport, particularly when infused near DA terminals (Masamizu et
508 al., 2011; Löw et al., 2013). However, using TH immunohistochemistry, we did not detect GCaMP6s
509 expression in either DA terminals in the NAc or in DA cell bodies in the VTA (data not shown).
510
511 **Conclusions**
512 Together, these data highlight a central role for NAc dMSN, iMSN, and DA signaling in the acquisition and
513 expression of heroin CPP. Future work will investigate the role of NAc signaling in encoding individual
514 vulnerability to the rewarding and motivating effects of heroin, with a particular focus on the relative
515 strength of dMSNs and iMSNs between individuals sensitive to versus resistant to the conditioned
516 reinforcement produced by heroin.

REFERENCES

Albin, R. L., Young, A. B., and Penney, J. B. (1989). The functional anatomy of basal ganglia disorders. *Trends Neurosci.* doi:10.1016/0166-2236(89)90074-X.

Badiani, A., Belin, D., Epstein, D., Calu, D., and Shaham, Y. (2011). Opiate versus psychostimulant addiction: The differences do matter. *Nat. Rev. Neurosci.* doi:10.1038/nrn3104.

Bailey, C. H., Giustetto, M., Huang, Y. Y., Hawkins, R. D., and Kandel, E. R. (2000). Is Heterosynaptic modulation essential for stabilizing hebbian plasiticity and memory. *Nat. Rev. Neurosci.* doi:10.1038/35036191.

Bardo, M. T., Rowlett, J. K., and Harris, M. J. (1995). Conditioned place preference using opiate and stimulant drugs: A meta-analysis. *Neurosci. Biobehav. Rev.* doi:10.1016/0149-7634(94)00021-R.

Belin, D., Mar, A. C., Dalley, J. W., Robbins, T. W., and Everitt, B. J. (2008). High impulsivity predicts the switch to compulsive cocaine-taking. *Science (80-.).* doi:10.1126/science.1158136.

Bock, R., Hoon Shin, J., Kaplan, A. R., Dobi, A., Markey, E., Kramer, P. F., et al. (2013). Strengthening the accumbal indirect pathway promotes resilience to compulsive cocaine use. *Nat. Neurosci.* doi:10.1038/nn.3369.

Burke, D. A., Rotstein, H. G., and Alvarez, V. A. (2017). Striatal Local Circuitry: A New Framework for Lateral Inhibition. *Neuron.* doi:10.1016/j.neuron.2017.09.019.

Calabresi, P., Picconi, B., Tozzi, A., Ghiglieri, V., and Di Filippo, M. (2014). Direct and indirect pathways of basal ganglia: A critical reappraisal. *Nat. Neurosci.* doi:10.1038/nn.3743.

Calipari, E. S., Bagot, R. C., Purushothaman, I., Davidson, T. J., Yorgason, J. T., Peña, C. J., et al. (2016). In vivo imaging identifies temporal signature of D1 and D2 medium spiny neurons in cocaine reward. *Proc. Natl. Acad. Sci. U. S. A.* doi:10.1073/pnas.1521238113.

Carroll, M. E., and Lac, S. T. (1992). Effects of buprenorphine on self-administration of cocaine and a nondrug reinforcer in rats. *Psychopharmacology (Berl).* doi:10.1007/BF02244812.

Corre, J., van Zessen, R., Loureiro, M., Patriarchi, T., Tian, L., Pascoli, V., et al. (2018). Dopamine neurons projecting to medial shell of the nucleus accumbens drive heroin reinforcement. *Elife.* doi:10.7554/eLife.39945.

544 Creed, M., Kaufling, J., Fois, G. R., Jalabert, M., Yuan, T., Lüscher, C., et al. (2016). Cocaine exposure
545 enhances the activity of ventral tegmental area dopamine neurons via calcium-impermeable
546 NMDARs. *J. Neurosci.* doi:10.1523/JNEUROSCI.1703-16.2016.
547 Crummy, E. A., O'Neal, T. J., Baskin, B. M., and Ferguson, S. M. (2020). One Is Not Enough:
548 Understanding and Modeling Polysubstance Use. *Front. Neurosci.* 14.
549 doi:10.3389/fnins.2020.00569.
550 Cui, G., Jun, S. B., Jin, X., Pham, M. D., Vogel, S. S., Lovinger, D. M., et al. (2013). Concurrent activation
551 of striatal direct and indirect pathways during action initiation. *Nature*. doi:10.1038/nature11846.
552 Dobbs, L. K. K., Kaplan, A. R. R., Lemos, J. C. C., Matsui, A., Rubinstein, M., and Alvarez, V. A. A.
553 (2016). Dopamine Regulation of Lateral Inhibition between Striatal Neurons Gates the Stimulant
554 Actions of Cocaine. *Neuron*. doi:10.1016/j.neuron.2016.04.031.
555 Everitt, B. J., Giuliano, C., and Belin, D. (2018). Addictive behaviour in experimental animals: Prospects
556 for translation. *Philos. Trans. R. Soc. B Biol. Sci.* doi:10.1098/rstb.2017.0027.
557 Ferguson, S. M., Eskenazi, D., Ishikawa, M., Wanat, M. J., Phillips, P. E. M., Dong, Y., et al. (2011).
558 Transient neuronal inhibition reveals opposing roles of indirect and direct pathways in sensitization.
559 *Nat. Neurosci.* doi:10.1038/nn.2703.
560 Gerfen, C. R., and Surmeier, D. J. (2011). Modulation of Striatal Projection Systems by Dopamine. *Annu.*
561 *Rev. Neurosci.* doi:10.1146/annurev-neuro-061010-113641.
562 Grimm, J. W., Hope, B. T., Wise, R. A., and Shaham, Y. (2001). Incubation of cocaine craving after
563 withdrawal. *Nature*. doi:10.1038/35084134.
564 Hedegaard, H., Miniño, A. M., and Warner, M. (2018). Drug Overdose Deaths in the United States, 1999-
565 2017. *NCHS Data Brief*.
566 Isaacs, D. P., Leman, R. P., Everett, T. J., Lopez-Beltran, H., Hamilton, L. R., and Oleson, E. B. (2020).
567 Buprenorphine is a weak dopamine releaser relative to heroin, but its pretreatment attenuates
568 heroin-evoked dopamine release in rats. *Neuropsychopharmacol. Reports*. doi:10.1002/npr2.12139.
569 Johnson, S. W., and North, R. A. (1992). Opioids excite dopamine neurons by hyperpolarization of local
570 interneurons. *J. Neurosci.* doi:10.1523/jneurosci.12-02-00483.1992.

571 Koob, G. F., and Volkow, N. D. (2016). Neurobiology of addiction: a neurocircuitry analysis. *The Lancet*
572 *Psychiatry*. doi:10.1016/S2215-0366(16)00104-8.
573 Kravitz, A. V., Freeze, B. S., Parker, P. R. L., Kay, K., Thwin, M. T., Deisseroth, K., et al. (2010).
574 Regulation of parkinsonian motor behaviours by optogenetic control of basal ganglia circuitry.
575 *Nature*. doi:10.1038/nature09159.
576 Kremer, E. J., Boutin, S., Chillon, M., and Danos, O. (2009). Canine Adenovirus Vectors: an Alternative
577 for Adenovirus-Mediated Gene Transfer. *J. Virol.* doi:10.1128/jvi.74.1.505-512.2000.
578 Kupchik, Y. M., Brown, R. M., Heinsbroek, J. A., Lobo, M. K., Schwartz, D. J., and Kalivas, P. W. (2015).
579 Coding the direct/indirect pathways by D1 and D2 receptors is not valid for accumbens projections.
580 *Nat. Neurosci.* doi:10.1038/nn.4068.
581 Lobo, M. K., Covington, H. E., Chaudhury, D., Friedman, A. K., Sun, H. S., Damez-Werno, D., et al.
582 (2010). Cell type - Specific loss of BDNF signaling mimics optogenetic control of cocaine reward.
583 *Science (80-.).* doi:10.1126/science.1188472.
584 Löw, K., Aebischer, P., and Schneider, B. L. (2013). Direct and retrograde transduction of nigral neurons
585 with AAV6, 8, and 9 and intraneuronal persistence of viral particles. *Hum. Gene Ther.*
586 doi:10.1089/hum.2012.174.
587 Luo, Z., Volkow, N. D., Heintz, N., Pan, Y., and Du, C. (2011). Acute cocaine induces fast activation of D1
588 receptor and progressive deactivation of D2 receptor striatal neurons: In vivo optical microprobe [Ca
589 2+] i imaging. *J. Neurosci.* doi:10.1523/JNEUROSCI.2369-11.2011.
590 Macpherson, T., Morita, M., and Hikida, T. (2014). Striatal direct and indirect pathways control decision-
591 making behavior. *Front. Psychol.* doi:10.3389/fpsyg.2014.01301.
592 Maldonado, R., Saiardi, A., Valverde, O., Samad, T. A., Roques, B. P., and Borrelli, E. (1997). Absence of
593 opiate, rewarding effects in mice lacking dopamine D2 receptors. *Nature*. doi:10.1038/41567.
594 Martianova, E., Aronson, S., and Proulx, C. D. (2019). Multi-fiber photometry to record neural activity in
595 freely-moving animals. *J. Vis. Exp.* doi:10.3791/60278.
596 Masamizu, Y., Okada, T., Kawasaki, K., Ishibashi, H., Yuasa, S., Takeda, S., et al. (2011). Local and
597 retrograde gene transfer into primate neuronal pathways via adeno-associated virus serotype 8 and

598 9. *Neuroscience*. doi:10.1016/j.neuroscience.2011.06.080.

599 Meng, C., Zhou, J., Papaneri, A., Peddada, T., Xu, K., and Cui, G. (2018). Spectrally Resolved Fiber
600 Photometry for Multi-component Analysis of Brain Circuits. *Neuron*.
601 doi:10.1016/j.neuron.2018.04.012.

602 Nader, M. A., Morgan, D., Gage, H. D., Nader, S. H., Calhoun, T. L., Buchheimer, N., et al. (2006). PET
603 imaging of dopamine D2 receptors during chronic cocaine self-administration in monkeys. *Nat.*
604 *Neurosci.* doi:10.1038/nn1737.

605 O'Neal, T. J., Nooney, M. N., Thien, K., and Ferguson, S. M. (2020). Chemogenetic modulation of
606 accumbens direct or indirect pathways bidirectionally alters reinstatement of heroin-seeking in high-
607 but not low-risk rats. *Neuropsychopharmacology* 45, 1251–1262. doi:10.1038/s41386-019-0571-9.

608 Park, K., Volkow, N. D., Pan, Y., and Du, C. (2013). Chronic cocaine dampens dopamine signaling during
609 cocaine intoxication and unbalances D1 over D2 receptor signaling. *J. Neurosci.*
610 doi:10.1523/JNEUROSCI.1935-13.2013.

611 Patriarchi, T., Cho, J. R., Merten, K., Howe, M. W., Marley, A., Xiong, W. H., et al. (2018). Ultrafast
612 neuronal imaging of dopamine dynamics with designed genetically encoded sensors. *Science (80-.*
613 *).* doi:10.1126/science.aat4422.

614 Paxinos, G., Watson, C. R. R., and Emson, P. C. (1980). AChE-stained horizontal sections of the rat brain
615 in stereotaxic coordinates. *J. Neurosci. Methods*. doi:10.1016/0165-0270(80)90021-7.

616 Phillips, P. E. M., Stuber, G. D., Helen, M. L. A. V., Wightman, R. M., and Carelli, R. M. (2003).
617 Subsecond dopamine release promotes cocaine seeking. *Nature*. doi:10.1038/nature01476.

618 Plotkin, J. L., Shen, W., Rafalovich, I., Sebel, L. E., Day, M., Savio Chan, C., et al. (2013). Regulation of
619 dendritic calcium release in striatal spiny projection neurons. *J. Neurophysiol.*
620 doi:10.1152/jn.00422.2013.

621 Proulx, C. D., Aronson, S., Milivojevic, D., Molina, C., Loi, A., Monk, B., et al. (2018). A neural pathway
622 controlling motivation to exert effort. *Proc. Natl. Acad. Sci. U. S. A.* doi:10.1073/pnas.1801837115.

623 Sellings, L. H. L., and Clarke, P. B. S. (2003). Segregation of amphetamine reward and locomotor
624 stimulation between nucleus accumbens medial shell and core. *J. Neurosci.*

doi:10.1523/jneurosci.23-15-06295.2003.

Shaham, Y., Shalev, U., Lu, L., De Wit, H., and Stewart, J. (2003). The reinstatement model of drug relapse: History, methodology and major findings. *Psychopharmacology (Berl).* doi:10.1007/s00213-002-1224-x.

Shippenberg, T. S., Bals-Kubik, R., and Herz, A. (1993). Examination of the neurochemical substrates mediating the motivational effects of opioids: Role of the mesolimbic dopamine system and D-1 vs. D-2 dopamine receptors. *J. Pharmacol. Exp. Ther.*

Stinus, L., Nadaud, D., Deminière, J. M., Jauregui, J., Hand, T. T., and Le Moal, M. (1989). Chronic flupentixol treatment potentiates the reinforcing properties of systemic heroin administration. *Biol. Psychiatry*. doi:10.1016/0006-3223(89)90052-8.

Swapna, I., Bondy, B., and Morikawa, H. (2016). Differential Dopamine Regulation of Ca2+ Signaling and Its Timing Dependence in the Nucleus Accumbens. *Cell Rep.* doi:10.1016/j.celrep.2016.03.055.

Taverna, S., Ilijic, E., and Surmeier, D. J. (2008). Recurrent collateral connections of striatal medium spiny neurons are disrupted in models of Parkinson's disease. *J. Neurosci.* doi:10.1523/JNEUROSCI.5493-07.2008.

Tervo, D. G. R., Hwang, B. Y., Viswanathan, S., Gaj, T., Lavzin, M., Ritola, K. D., et al. (2016). A Designer AAV Variant Permits Efficient Retrograde Access to Projection Neurons. *Neuron*. doi:10.1016/j.neuron.2016.09.021.

Volkow, N. D., Wang, G. J., Fowler, J. S., Thanos, P., Logan, J., Gatley, S. J., et al. (2002). Brain DA D2 receptors predict reinforcing effects of stimulants in humans: Replication study. *Synapse*. doi:10.1002/syn.10137.

Yager, L. M., Garcia, A. F., Donckels, E. A., and Ferguson, S. M. (2019). Chemogenetic inhibition of direct pathway striatal neurons normalizes pathological, cue-induced reinstatement of drug-seeking in rats. *Addict. Biol.* doi:10.1111/adb.12594.

651 **FIGURE LEGENDS**

652

653 **Figure 1 | Expression of heroin CPP is accompanied with NAc activation**

654 ***A***, Timeline for heroin CPP procedure. Rats underwent two preference tests (15 min each) separated by
655 eight conditioning sessions (2x/day, 40 min each), and activation of the NAc during the post-test was
656 assessed via Fos immunohistochemistry. ***B-C***, Rats conditioned with 3 mg/kg heroin spent more time in
657 the heroin-paired chamber during the post-test and developed a significant preference for the heroin-
658 paired chamber. ***D-E***, Representative images and quantification of Fos in the NAc core. ***F-G***,
659 Representative images and quantification of Fos in the NAc shell. n = 8/group; scale bar = 50 μm; *p <
660 .05, **p < .01

661

662 **Figure 2 | Experimental design for fiber photometry recordings in the NAc**. ***A***, Timeline for
663 photometry recordings prior to CPP. Rats underwent brief (~5 min) recordings in their home cages to
664 verify signal quality. ***B***, Experimental setup. Rats were connected to a fiber photometry system via a
665 branching fiber optic patch cord for *in vivo* recordings. ***C***, LED configuration for single or dual color
666 imaging with interleaved isosbestic wavelength. ***D-E***, Viral strategy for dopamine imaging and expression
667 of dLight1.3b throughout the NAc. ***F***, Representative dLight expression with TH staining of DA terminals
668 in the NAc. ***G-H***, Viral strategy for dMSN/iMSN imaging and expression of GCaMP6s and RCaMP1b
669 throughout the NAc. ***I***, Representative GCaMP and RCaMP expression in the NAc. ***J***, Analysis pipeline
670 for photometry data. Raw signals were de-interleaved to separate channels, then linearized and
671 converted to z-scores. Events were detected and extracted from normalized signals, and event
672 characteristics were examined. +: optic fiber location; TH: tyrosine hydroxylase; scale bar = 100 μm

673

674 **Figure 3 | Heroin conditioning disrupts DA, dMSN, and iMSN signaling in the NAc**. ***A-B***, Timeline
675 and experimental design for photometry recordings during CPP conditioning sessions. ***C, H, M***,
676 Representative signals collected during conditioning. ***C-D***, Heroin reduced the frequency of DA events in
677 session 1 but increased the frequency of DA events in session 4. ***E-G***, Heroin reduced the frequency of

678 large amplitude DA events, the average amplitude of DA events, and the variance of DA event
679 amplitudes. ***H-I***, The frequency of dMSN events after the fourth saline pairing was significantly lower than
680 after the first saline pairing. ***J-L***, Heroin reduced the proportion of large dMSN events and the average
681 amplitude of dMSN events but had no effect on the variance of dMSN events. ***M-N***, Heroin increased the
682 frequency of iMSN events in session 1 but reduced the frequency of iMSN events in session 4. ***O-P***,
683 Heroin increased the proportion of large amplitude iMSN events and the average amplitude of iMSN
684 events in session 1 but decreased the proportion of large amplitude iMSN events and the average
685 amplitude of iMSN events in session 4. ***Q***, The variance of iMSN events was unchanged during
686 conditioning. n = 9-12 rats; *$p < .05$, **$p < .01$, ***$p < .001$, ****$p < .0001$ (saline vs heroin); ##$p < .01$, ###p
687 $< .001$ (session 1 vs session 4)
688
689 **Figure 4 l Increased DA signaling precedes entry to a heroin-paired context**. ***A-B***, Timeline and
690 strategy for NAc DA recordings during CPP test sessions, and representative DA traces collected during
691 the pre- and post-test. ***C***, Rats significantly increased preference for the heroin-paired chamber after
692 conditioning. ***D-O***, NAc DA signals aligned to transitions in the CPP chamber. Following conditioning, ***D-F***,
693 DA signaling was significantly attenuated when entering the saline-paired chamber and ***G-I***, unchanged
694 when exiting the saline-paired chamber. Following conditioning, ***J-L***, DA signaling was significantly
695 enhanced when entering the heroin-paired chamber and ***M-O***, significantly attenuated when exiting the
696 heroin-paired chamber. n = 9 rats; *$p < .05$, **$p < .01$, ***$p < .001$, ****$p < .0001$
697
698 **Figure 5 l Increased dMSN signaling precedes entry to a heroin-paired context**. ***A-B***, Timeline and
699 strategy for NAc dMSN recordings during CPP test sessions, and representative dMSN traces collected
700 during the pre- and post-test. ***C***, Rats significantly increased preference for the heroin-paired chamber
701 after conditioning. ***D-O***, NAc dMSN signals aligned to transitions in the CPP chamber. Following
702 conditioning, ***D-F***, dMSN signaling was significantly attenuated when entering the saline-paired chamber
703 and ***G-I***, unchanged when exiting the saline-paired chamber. Following conditioning, ***J-L***, dMSN signaling

was significantly enhanced when entering the heroin-paired chamber and ***M-O***, significantly attenuated when exiting the heroin-paired chamber. $n = 12$ rats; $^{**}p < .01$, $^{***}p < .001$, $^{****}p < .0001$

Figure 6 | Decreased iMSN signaling precedes entry to a heroin-paired context. ***A-B***, Timeline and strategy for NAc iMSN recordings during CPP test sessions, and representative iMSN traces collected during the pre- and post-test. ***C***, Rats significantly increased preference for the heroin-paired chamber after conditioning. ***D-O***, NAc iMSN signals aligned to transitions in the CPP chamber. Following conditioning, ***D-F***, iMSN signaling was significantly enhanced when entering the saline-paired chamber and ***G-I***, unchanged when exiting the saline-paired chamber. Following conditioning, ***J-L***, iMSN signaling was significantly attenuated when entering the heroin-paired chamber and ***M-O***, significantly enhanced when exiting the heroin-paired chamber. $n = 10$ rats; $^{*}p < .05$, $^{**}p < .01$

Figure *7* | Acquisition of heroin CPP is blocked by buprenorphine. ***A***, Timeline for buprenorphine experiment. Testing was performed as described in **Figure 1**, but rats received buprenorphine pretreatment 10 min prior to each conditioning session. ***B-C***, Rats pretreated with 0.2 mg/kg buprenorphine spent significantly less time in the heroin-paired chamber during the post-test than those pretreated with 0 mg/kg buprenorphine and did not develop a preference for the heroin-paired chamber. ***D-G***, Representative images and quantification of Fos in the NAc. Rats pretreated with 0.2 mg/kg buprenorphine had significantly less Fos in both subregions of the NAc than those pretreated with 0 mg/kg buprenorphine. $n = 8$/group; scale bar = 50 μm; $^{*}p < .05$, $^{**}p < .01$, $^{***}p < .001$, $^{****}p < .0001$

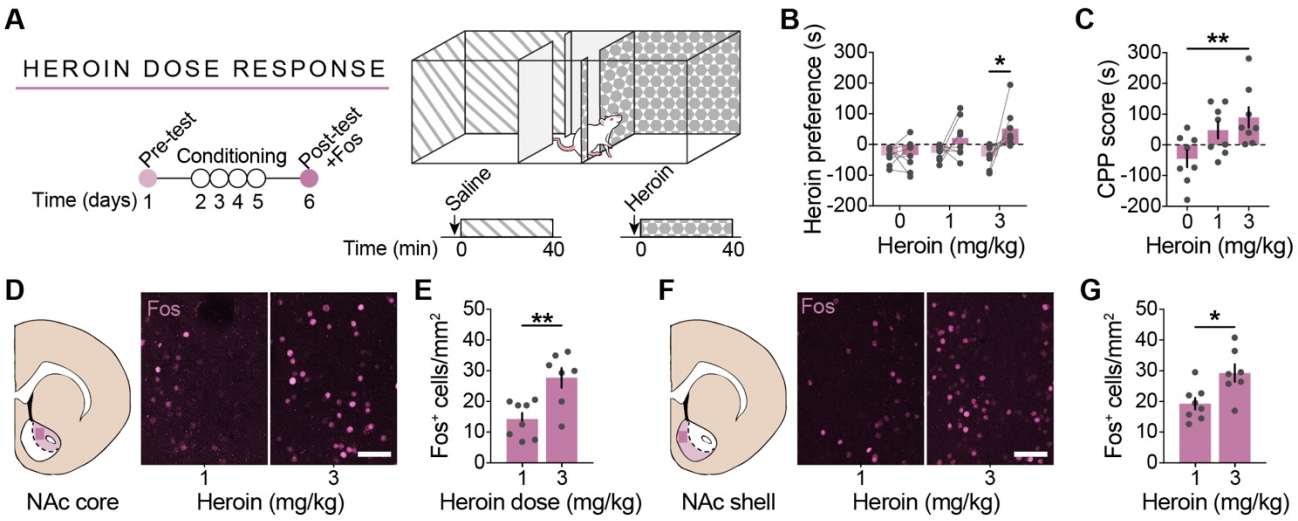

724 **Figure 1 | Expression of heroin CPP is accompanied with NAc activation**

725 ***A***, Timeline for heroin CPP procedure. Rats underwent two preference tests (15 min each) separated by
726 eight conditioning sessions (2x/day, 40 min each), and activation of the NAc during the post-test was
727 assessed via Fos immunohistochemistry. ***B-C***, Rats conditioned with 3 mg/kg heroin spent more time in
728 the heroin-paired chamber during the post-test and developed a significant preference for the heroin-
729 paired chamber. ***D-E***, Representative images and quantification of Fos in the NAc core. ***F-G***,
730 Representative images and quantification of Fos in the NAc shell. n = 8/group; scale bar = 50 μm; *p <
731 .05, **p < .01

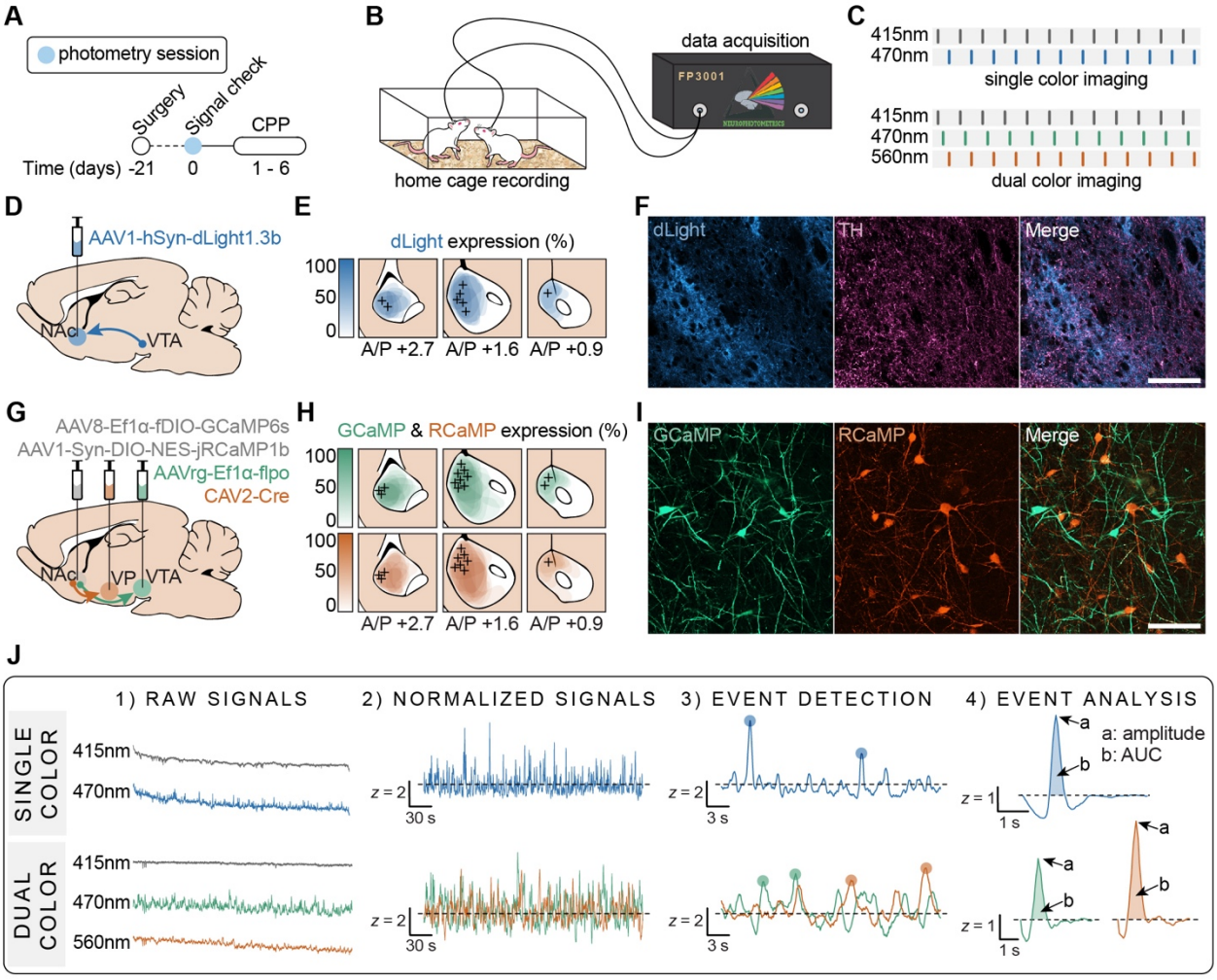

Figure 2 | Experimental design for fiber photometry recordings in the NAc. ***A***, Timeline for photometry recordings prior to CPP. Rats underwent brief (~5 min) recordings in their home cages to verify signal quality. ***B***, Experimental setup. Rats were connected to a fiber photometry system via a branching fiber optic patch cord for *in vivo* recordings. ***C***, LED configuration for single or dual color imaging with interleaved isosbestic wavelength. ***D-E***, Viral strategy for dopamine imaging and expression of dLight1.3b throughout the NAc. ***F***, Representative dLight expression with TH staining of DA terminals in the NAc. ***G-H***, Viral strategy for dMSN/iMSN imaging and expression of GCaMP6s and RCaMP1b throughout the NAc. ***I***, Representative GCaMP and RCaMP expression in the NAc. ***J***, Analysis pipeline for photometry data. Raw signals were de-interleaved to separate channels, then linearized and converted to z-scores. Events were detected and extracted from normalized signals, and event characteristics were examined. +: optic fiber location; TH: tyrosine hydroxylase; scale bar = 100 μm

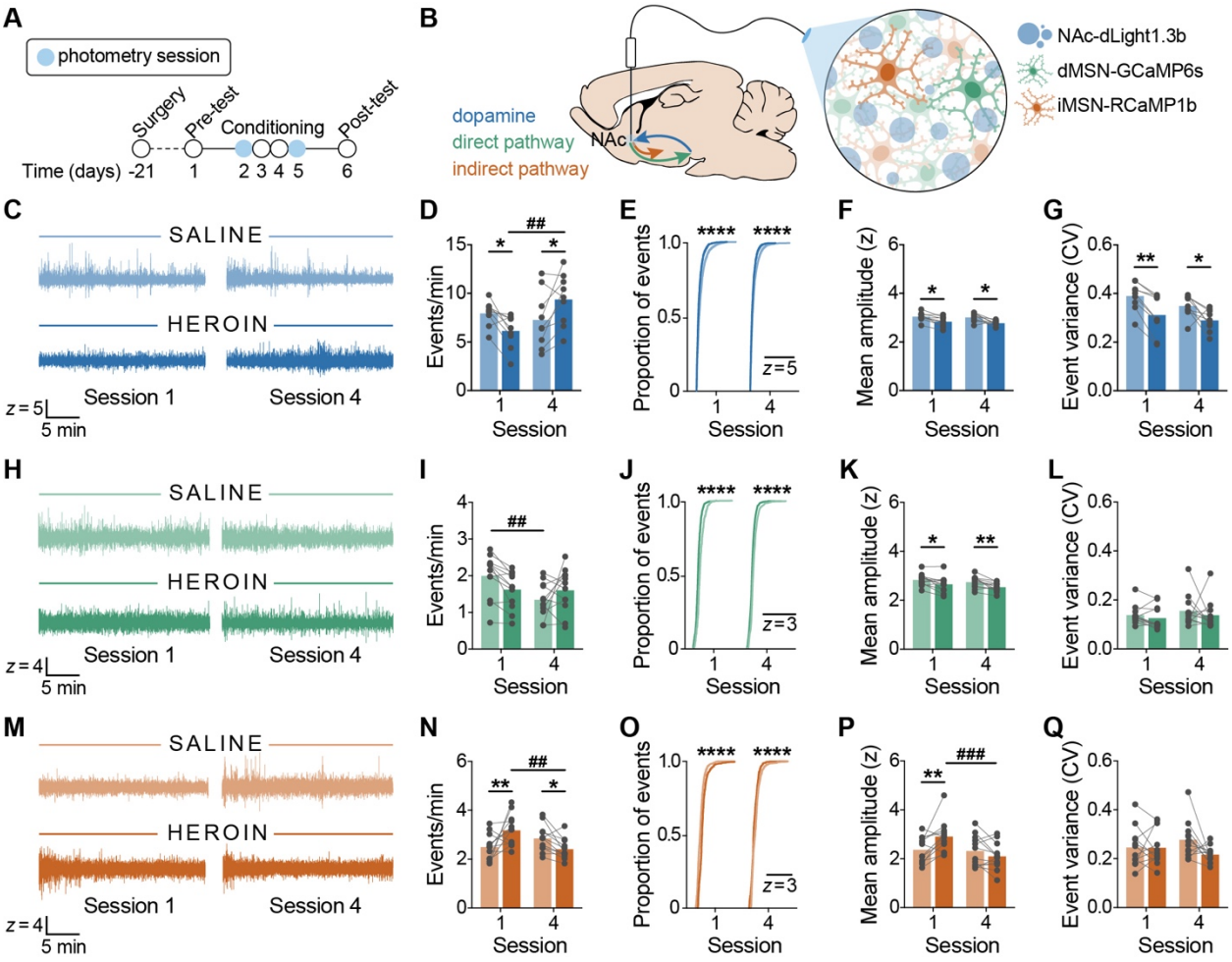

744

745 **Figure 3 l Heroin conditioning disrupts DA, dMSN, and iMSN signaling in the NAc**. ***A-B***, Timeline
746 and experimental design for photometry recordings during CPP conditioning sessions. ***C, H, M***,
747 Representative signals collected during conditioning. ***C-D***, Heroin reduced the frequency of DA events in
748 session 1 but increased the frequency of DA events in session 4. ***E-G***, Heroin reduced the frequency of
749 large amplitude DA events, the average amplitude of DA events, and the variance of DA event
750 amplitudes. ***H-I***, The frequency of dMSN events after the fourth saline pairing was significantly lower than
751 after the first saline pairing. ***J-L***, Heroin reduced the proportion of large dMSN events and the average
752 amplitude of dMSN events but had no effect on the variance of dMSN events. ***M-N***, Heroin increased the
753 frequency of iMSN events in session 1 but reduced the frequency of iMSN events in session 4. ***O-P***,
754 Heroin increased the proportion of large amplitude iMSN events and the average amplitude of iMSN
755 events in session 1 but decreased the proportion of large amplitude iMSN events and the average

amplitude of iMSN events in session 4. ***Q***, The variance of iMSN events was unchanged during conditioning. n = 9-12 rats; *$p < .05$, **$p < .01$, ***$p < .001$, ****$p < .0001$ (saline vs heroin); $^{\#\#}p < .01$, $^{\#\#\#}p < .001$ (session 1 vs session 4)

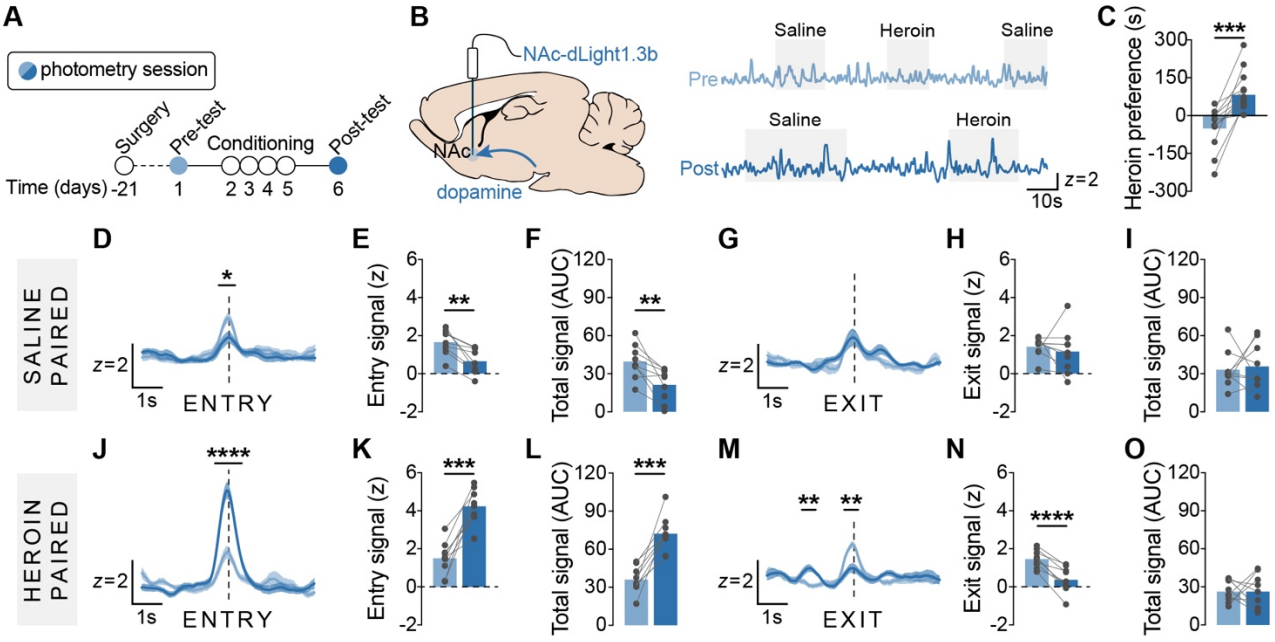

Figure 4 | Increased DA signaling precedes entry to a heroin-paired context. ***A-B***, Timeline and strategy for NAc DA recordings during CPP test sessions, and representative DA traces collected during the pre- and post-test. ***C***, Rats significantly increased preference for the heroin-paired chamber after conditioning. ***D-O***, NAc DA signals aligned to transitions in the CPP chamber. Following conditioning, ***D-F***, DA signaling was significantly attenuated when entering the saline-paired chamber and ***G-I***, unchanged when exiting the saline-paired chamber. Following conditioning, ***J-L***, DA signaling was significantly enhanced when entering the heroin-paired chamber and ***M-O***, significantly attenuated when exiting the heroin-paired chamber. $n = 9$ rats; $^{*}p < .05$, $^{**}p < .01$, $^{***}p < .001$, $^{****}p < .0001$

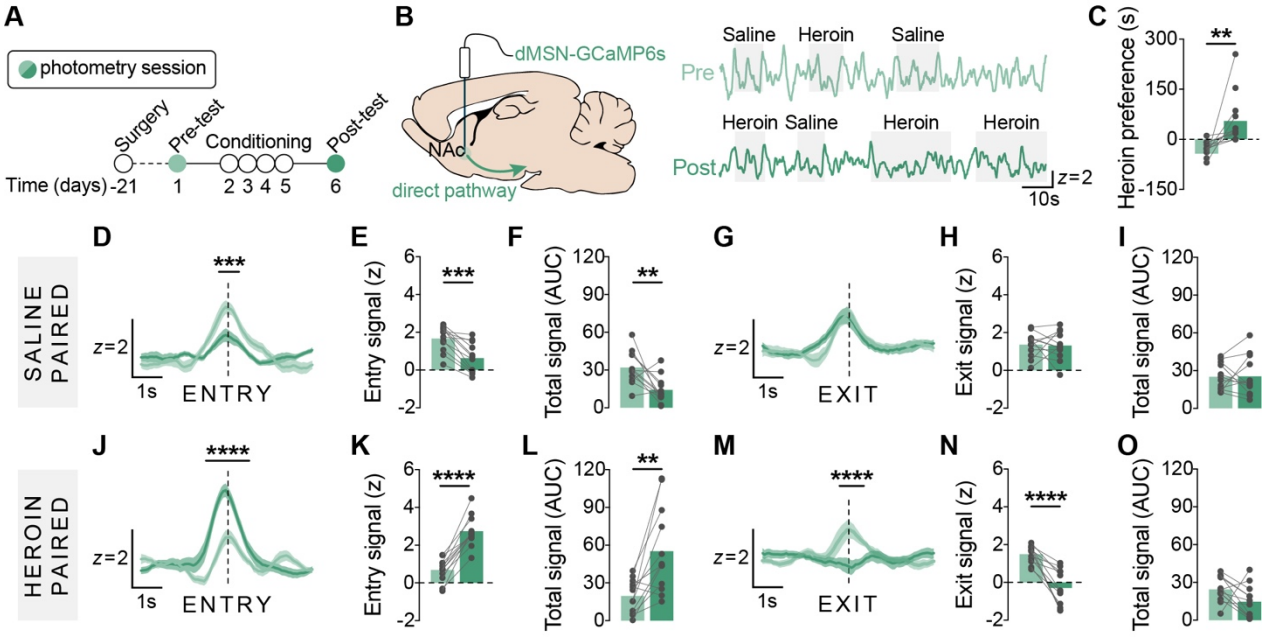

768

769 **Figure 5 | Increased dMSN signaling precedes entry to a heroin-paired context**. ***A-B***, Timeline and
770 strategy for NAc dMSN recordings during CPP test sessions, and representative dMSN traces collected
771 during the pre- and post-test. ***C***, Rats significantly increased preference for the heroin-paired chamber
772 after conditioning. ***D-O***, NAc dMSN signals aligned to transitions in the CPP chamber. Following
773 conditioning, ***D-F***, dMSN signaling was significantly attenuated when entering the saline-paired chamber
774 and ***G-I***, unchanged when exiting the saline-paired chamber. Following conditioning, ***J-L***, dMSN signaling
775 was significantly enhanced when entering the heroin-paired chamber and ***M-O***, significantly attenuated
776 when exiting the heroin-paired chamber. $n = 12$ rats; $^{**}p < .01$, $^{***}p < .001$, $^{****}p < .0001$

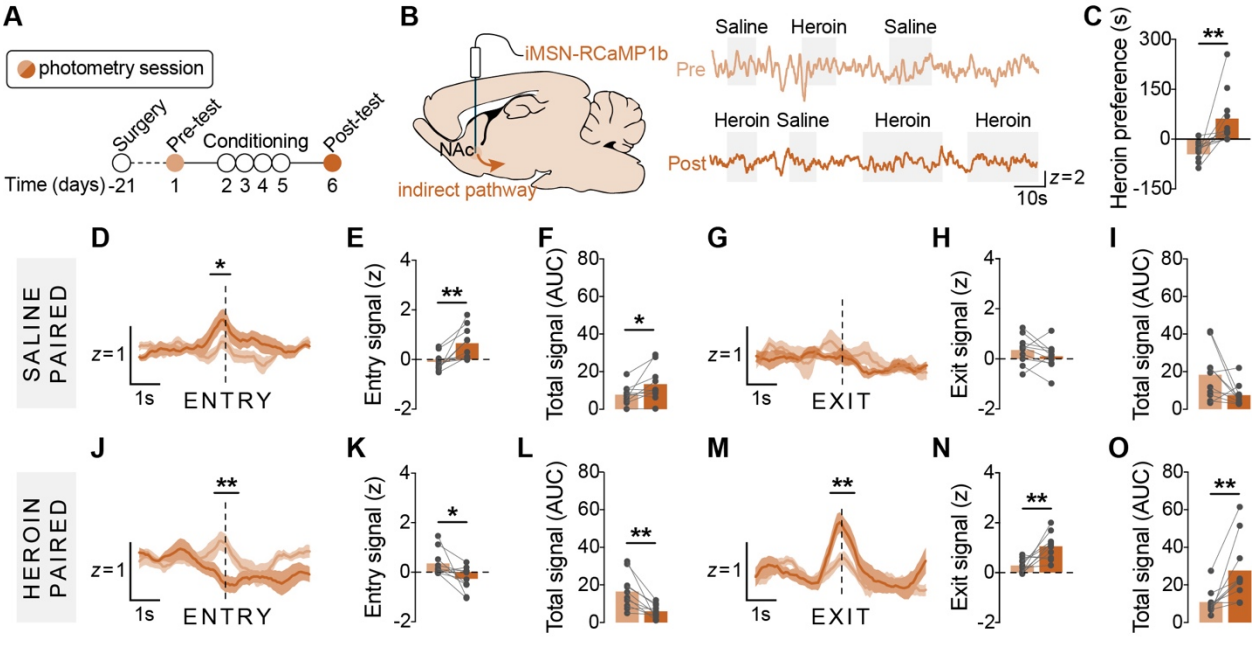

777

778 **Figure 6 | Decreased iMSN signaling precedes entry to a heroin-paired context**. ***A-B***, Timeline and
779 strategy for NAc iMSN recordings during CPP test sessions, and representative iMSN traces collected
780 during the pre- and post-test. ***C***, Rats significantly increased preference for the heroin-paired chamber
781 after conditioning. ***D-O***, NAc iMSN signals aligned to transitions in the CPP chamber. Following
782 conditioning, ***D-F***, iMSN signaling was significantly enhanced when entering the saline-paired chamber
783 and ***G-I***, unchanged when exiting the saline-paired chamber. Following conditioning, ***J-L***, iMSN signaling
784 was significantly attenuated when entering the heroin-paired chamber and ***M-O***, significantly enhanced
785 when exiting the heroin-paired chamber. $n = 10$ rats; $^{*}p < .05$, $^{**}p < .01$

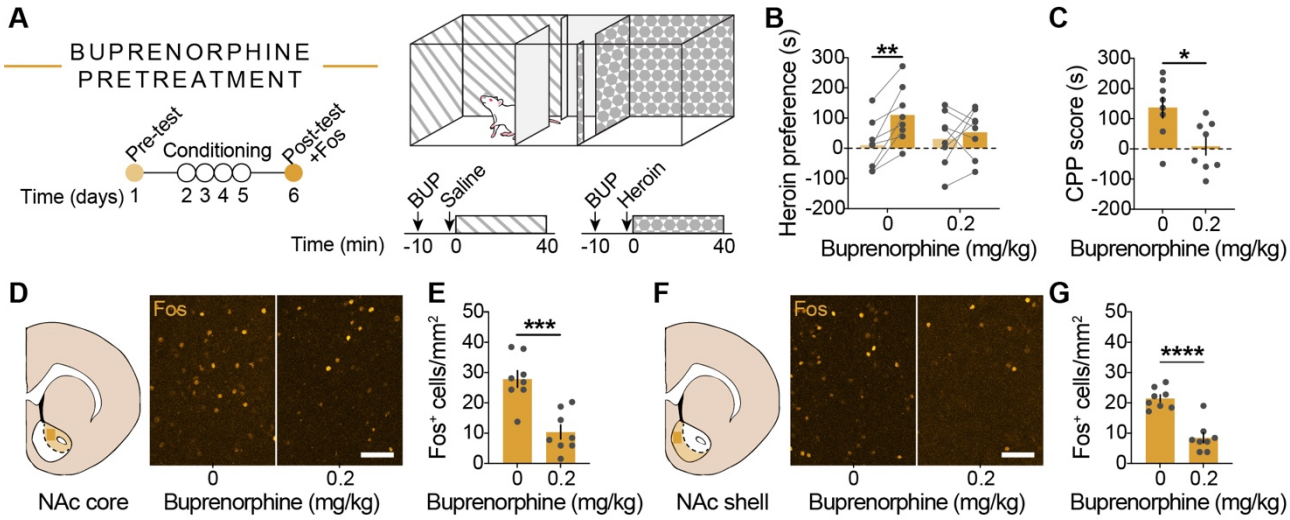

Figure 7 | Acquisition of heroin CPP is blocked by buprenorphine. ***A***, Timeline for buprenorphine experiment. Testing was performed as described in **Figure 1**, but rats received buprenorphine pretreatment 10 min prior to each conditioning session. ***B-C***, Rats pretreated with 0.2 mg/kg buprenorphine spent significantly less time in the heroin-paired chamber during the post-test than those pretreated with 0 mg/kg buprenorphine and did not develop a preference for the heroin-paired chamber. ***D-G***, Representative images and quantification of Fos in the NAc. Rats pretreated with 0.2 mg/kg buprenorphine had significantly less Fos in both subregions of the NAc than those pretreated with 0 mg/kg buprenorphine. *n* = 8/group; scale bar = 50 μm; **p* < .05, ***p* < .01, ****p* < .001, *****p* < .0001

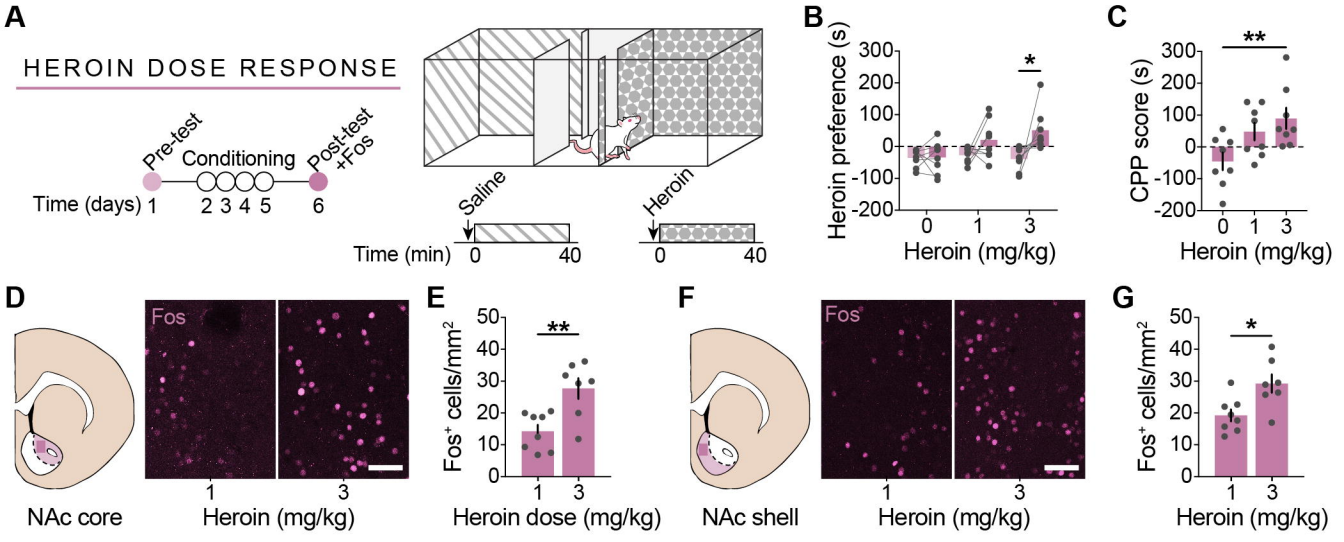
A
HEROIN DOSE RESPONSE
Pre-test
Conditioning
Post-test +Fos
Time (days) 1 2 3 4 5 6
Saline
Heroin
Time (min) 0 40 0 40
B
Heroin preference (s)
300
200
100
0
-100
-200
*
0 1 3
Heroin (mg/kg)
C
CPP score (s)
300
200
100
0
-100
-200
**
0 1 3
Heroin (mg/kg)
D
Fos
NAc core
1 3
Heroin (mg/kg)
E
Fos+ cells/mm2
50
40
30
20
10
0
**
1 3
Heroin dose (mg/kg)
F
Fos
NAc shell
1 3
Heroin (mg/kg)
G
Fos+ cells/mm2
50
40
30
20
10
0
*
1 3
Heroin (mg/kg)

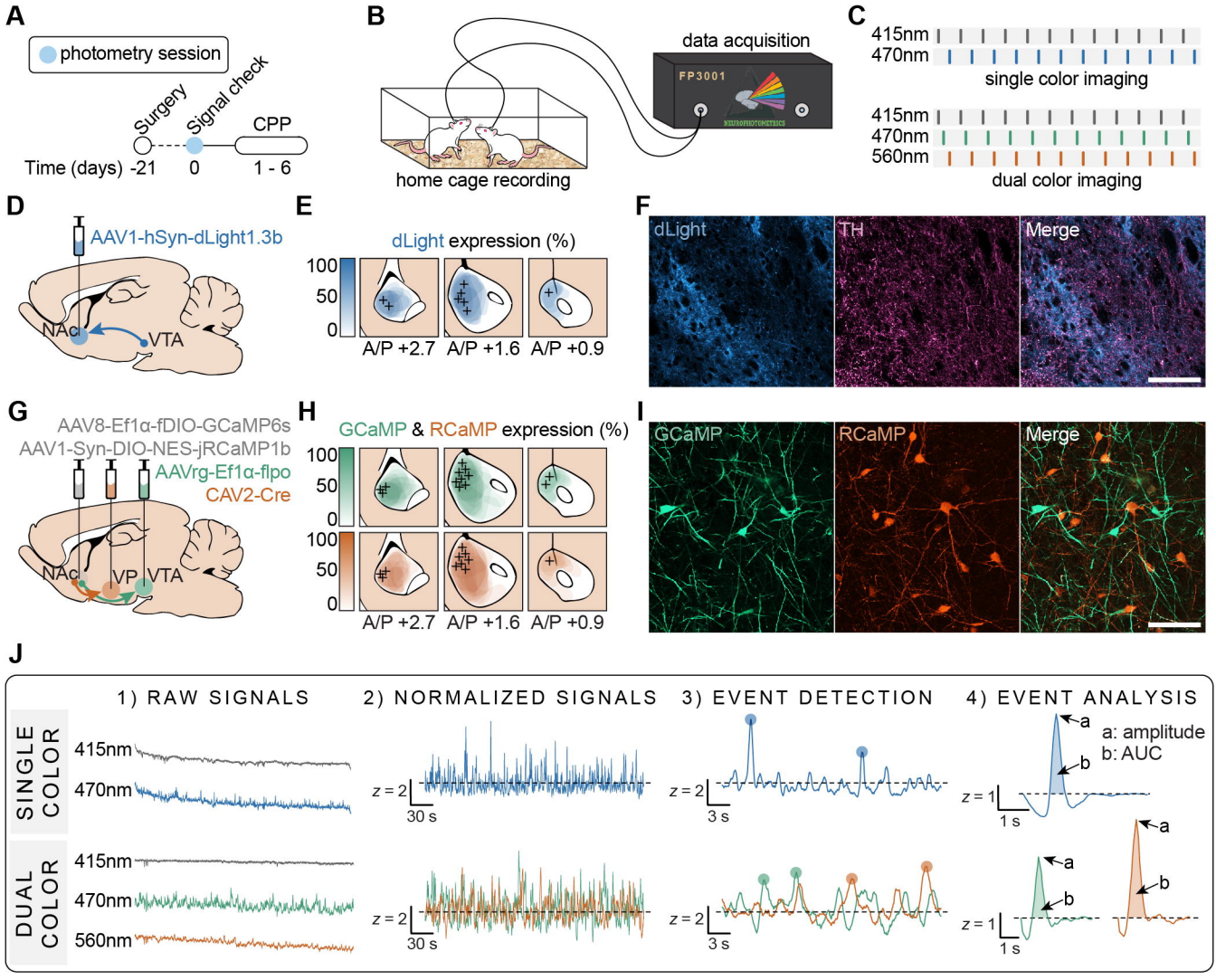
A
photometry session
Surgery
Signal check
CPP
Time (days) -21
0
1 - 6
B
data acquisition
FP3001
NEUROPHOTOMETRICS
home cage recording
C
415nm
470nm
single color imaging
415nm
470nm
560nm
dual color imaging
D
AAV1-hSyn-dLight1.3b
NAc
VTA
E
dLight expression (%)
100
50
0
A/P +2.7
A/P +1.6
A/P +0.9
F
dLight
TH
Merge
G
AAV8-Ef1α-fDIO-GCaMP6s
AAV1-Syn-DIO-NES-jRCaMP1b
AAVrg-Ef1α-flpo
CAV2-Cre
NAc
VP
VTA
H
GCaMP & RCaMP expression (%)
100
50
0
100
50
0
A/P +2.7
A/P +1.6
A/P +0.9
I
GCaMP
RCaMP
Merge
J
1) RAW SIGNALS
2) NORMALIZED SIGNALS
3) EVENT DETECTION
4) EVENT ANALYSIS
SINGLE COLOR
415nm
470nm
DUAL COLOR
415nm
470nm
560nm
z = 2
30 s
z = 2
3 s
a
b
a: amplitude
b: AUC
z = 1
1 s

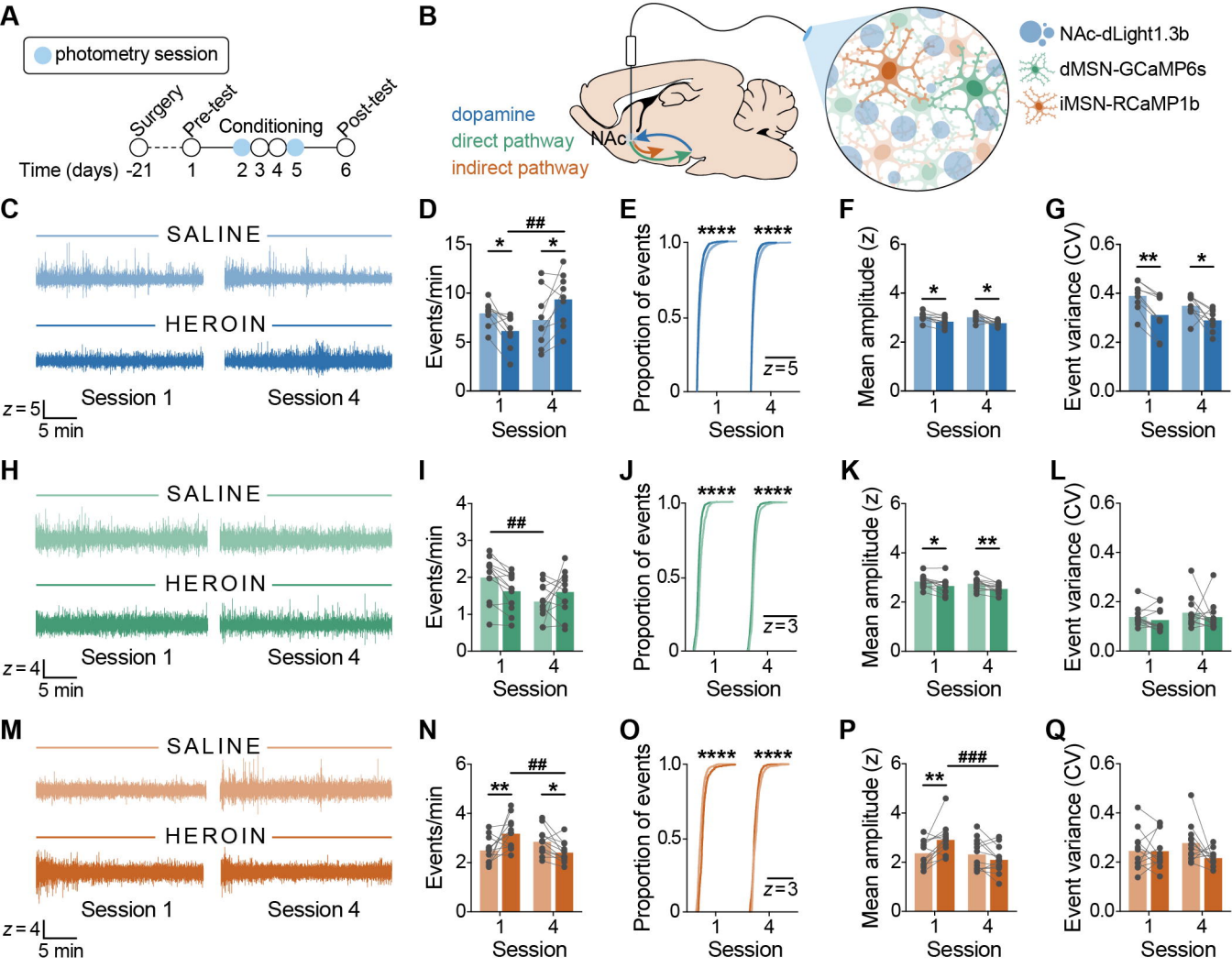
A
photometry session
Surgery
Pre-test
Conditioning
Post-test
Time (days) -21 1 2 3 4 5 6
B
dopamine
direct pathway
indirect pathway
NAc
NAc-dLight1.3b
dMSN-GCaMP6s
iMSN-RCaMP1b
C
SALINE
HEROIN
Session 1
Session 4
z = 5
5 min
D
Events/min
Session
E
Proportion of events
z=5
F
Mean amplitude (z)
G
Event variance (CV)
H
z = 4
I
z=3
K
L
M
N
O
P
Q

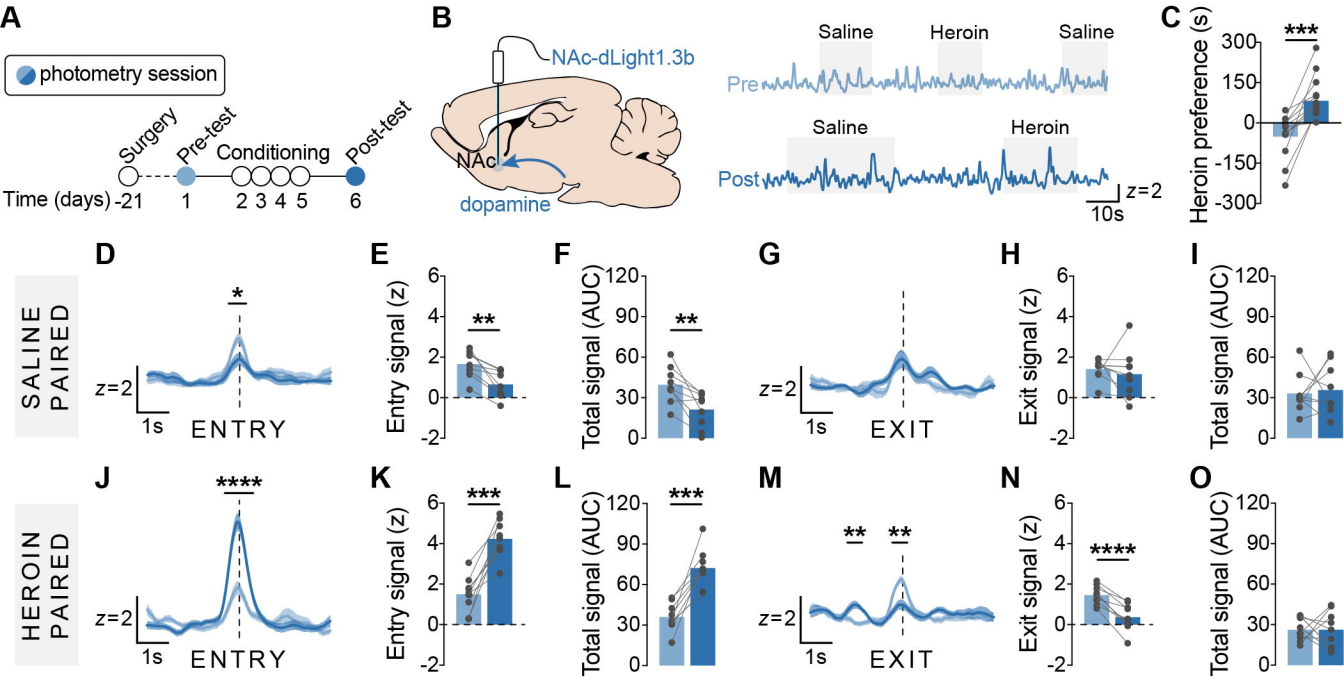
A
photometry session
Surgery
Pre-test
Conditioning
Post-test
Time (days) -21
1
2 3 4 5
6
B
NAc-dLight1.3b
NAc
dopamine
Saline
Heroin
Saline
Pre
Saline
Heroin
Post
z=2
10s
C
***
Heroin preference (s)
300
150
0
-150
-300
SALINE PAIRED
D
*
z=2
1s
ENTRY
E
**
Entry signal (z)
F
**
Total signal (AUC)
G
z=2
1s
EXIT
H
Exit signal (z)
I
Total signal (AUC)
HEROIN PAIRED
J
****
z=2
1s
ENTRY
K
***
Entry signal (z)
L
***
Total signal (AUC)
M
**
**
z=2
1s
EXIT
N
****
Exit signal (z)
O
Total signal (AUC)

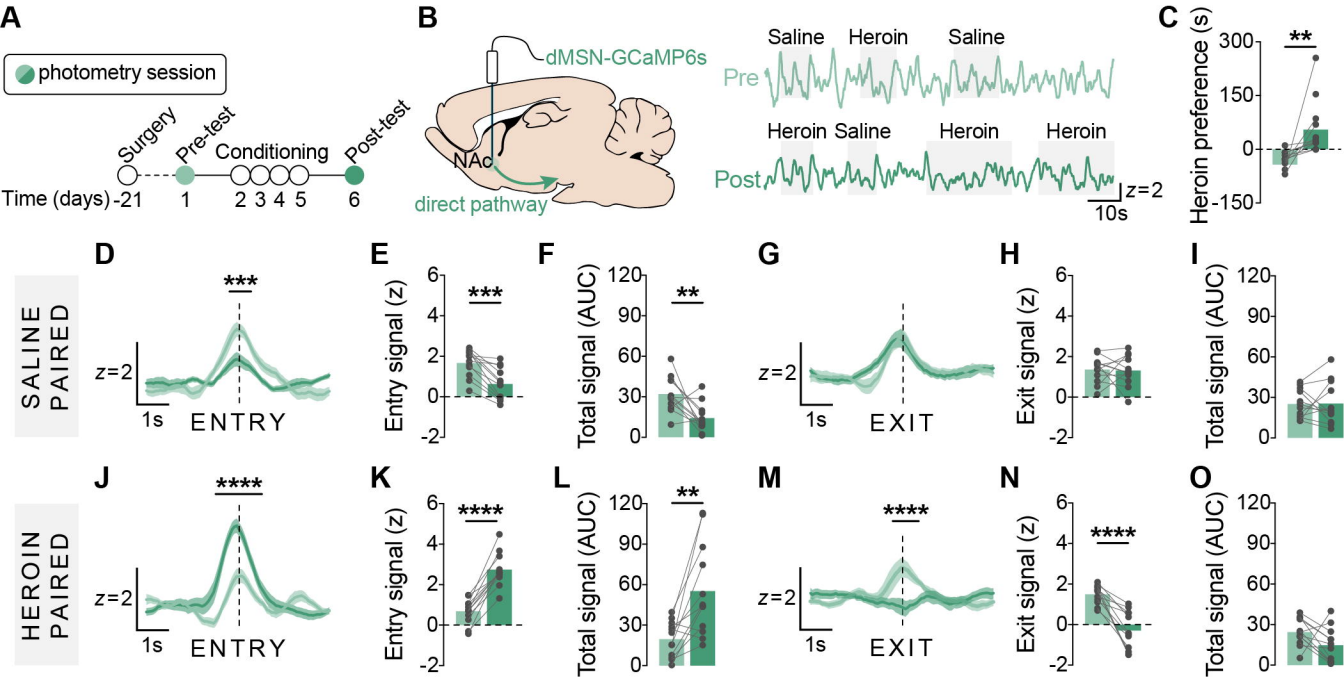
A
photometry session
Surgery
Pre-test
Conditioning
Post-test
Time (days) -21
1
2 3 4 5
6
B
dMSN-GCaMP6s
NAc
direct pathway
Saline
Heroin
Saline
Pre
Heroin
Saline
Heroin
Heroin
Post
z=2
10s
C
Heroin preference (s)
300
150
0
-150
**
SALINE PAIRED
D
***
z=2
1s
ENTRY
E
Entry signal (z)
***
F
Total signal (AUC)
**
G
z=2
1s
EXIT
H
Exit signal (z)
I
Total signal (AUC)
HEROIN PAIRED
J
****
z=2
1s
ENTRY
K
Entry signal (z)
****
L
Total signal (AUC)
**
M
****
z=2
1s
EXIT
N
Exit signal (z)
****
O
Total signal (AUC)

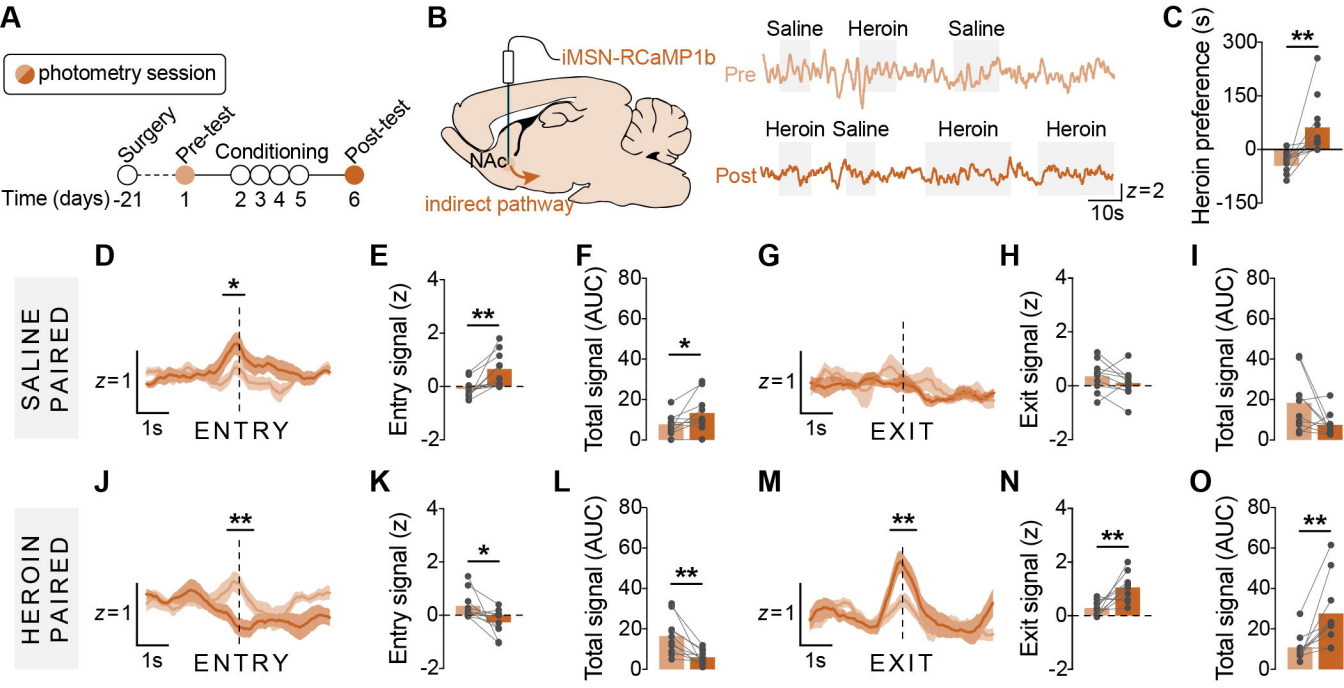
A
photometry session
Surgery
Pre-test
Conditioning
Post-test
Time (days) -21
1
2 3 4 5
6
B
iMSN-RCaMP1b
NAc
indirect pathway
Saline
Heroin
Saline
Pre
Heroin
Saline
Heroin
Heroin
Post
z=2
10s
C
Heroin preference (s)
300
150
0
-150
**
SALINE PAIRED
D
z=1
1s
ENTRY
*
E
Entry signal (z)
**
F
Total signal (AUC)
*
G
z=1
1s
EXIT
H
Exit signal (z)
I
Total signal (AUC)
HEROIN PAIRED
J
z=1
1s
ENTRY
**
K
Entry signal (z)
*
L
Total signal (AUC)
**
M
**
z=1
1s
EXIT
N
Exit signal (z)
**
O
Total signal (AUC)
**

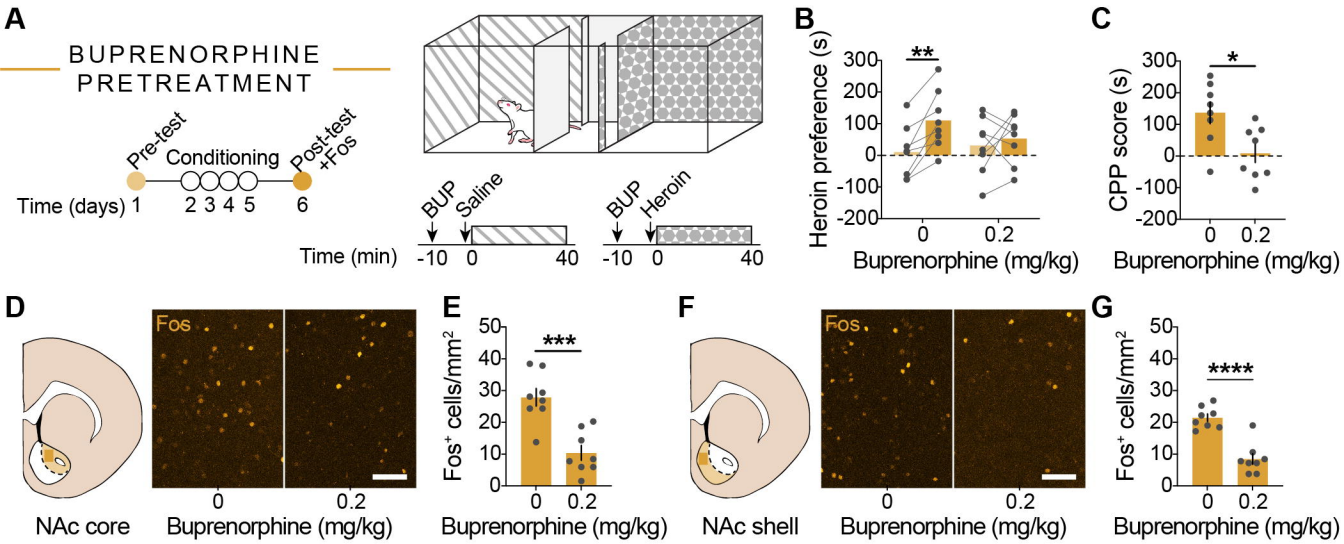
A
BUPRENORPHINE PRETREATMENT
Pre-test
Conditioning
Post-test +Fos
Time (days) 1 2 3 4 5 6
BUP
Saline
BUP
Heroin
Time (min) -10 0 40 -10 0 40
B
Heroin preference (s)
**
Buprenorphine (mg/kg)
C
CPP score (s)
*
Buprenorphine (mg/kg)
D
Fos
NAc core
Buprenorphine (mg/kg)
E
Fos+ cells/mm2
***
Buprenorphine (mg/kg)
F
Fos
NAc shell
Buprenorphine (mg/kg)
G
Fos+ cells/mm2
****
Buprenorphine (mg/kg)